Preparation and assessment of polylactic acid-curcumin nanofibrous wound dressing containing silver nanoparticles for burn wound treatment.

MOAYEDI, Mehri, AHMADI, Tahmineh, NEKOUIE, Vahid, DEHAGHANI, Majid Taghian, SHOJAEI, Shahrokh, BENISI, Soheila Zamalui and BAKHSHESHI-RAD, Hamid Reza

Highlights

1. Multifunctional PLA-Cur-AgNPs composite nanofiber were prepared using the electrospinning method.

2. PLA-Cur-AgNPs composite nanofiber results in superior antibacterial activity and cytocompatibility than PLA-Cur nanofiber.

3. Antibacterial performance of PLA-Cur-AgNPs composite nanofiber increases with increasing AgNPs concentration.

4. For wound healing and burn treatment, the PLA-Cur-AgNPs composite nanofiber is proposed.

Graphical Abstract

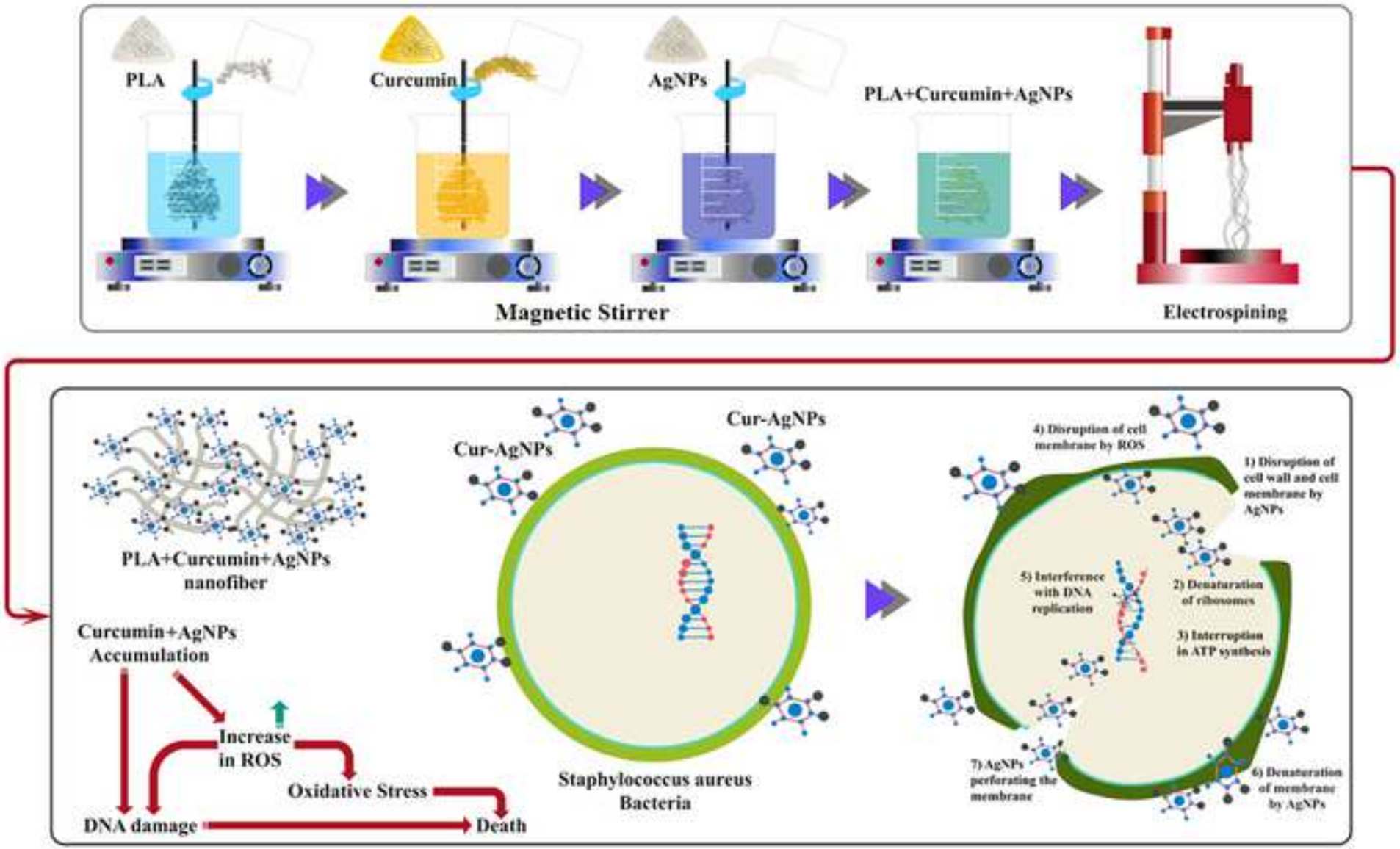

Preparation and assessment of polylactic acid-curcumin nanofibrous wound dressing containing silver nanoparticles for burn wound treatment

Mehri Moayedi [a], Tahmineh Ahmadi[a,*], Vahid Nekouie[b,c] , Majid Taghian Dehaghani[d], Shahrokh Shojaei[a], Soheila Zamalui Benisi[a,e] , Hamid Reza Bakhsheshi-Rad[f,*]

[a]Department of Biomedical Engineering, Islamic Azad University, Central Tehran Branch, P.O. Box 13185/768, Tehran, Iran
[b]Department of Engineering and Mathematics, Sheffield Hallam University, Sheffield, S1 1WB, UK
[c]Materials and Engineering Research Institute (MERI), Sheffield Hallam University, Sheffield, S1 1WB, UK
[d]Department of Materials and Metallurgical Engineering, Abadeh Higher Education Centre, Shiraz University, Abadeh, Iran
[e] Stem Cells Research Center, Tissue Engineering and regenerative Medicine Institute, Ventral Tehran Branch, Islamic Azad University, Tehran, Iran
[f]Advanced Materials Research Center, Department of Materials Engineering, Najafabad Branch, Islamic Azad University, Najafabad, Iran

*Correspondence: tahmadi56@yahoo.com (T.A); rezabakhsheshi@gmail.com (H.R.B.-R.)

Abstract

This study aims to produce and evaluate nanofibrous wound dressings through the electrospinning method, utilizing polylactic acid (PLA), curcumin (Cur), and silver nanoparticles (AgNPs). For this purpose, five types of wound dressings with PLA, PLA+Cur, PLA+Cur+1%AgNPs, PLA+Cur+2%AgNPs and PLA+Cur+3%AgNPs were produced using the electrospinning method. Analysis of the Fourier transform infrared spectroscopy and scanning electron microscopic observations indicated the successful fabrication, with nanometer diameters achieved in all electrospun samples. The examination of water absorption of wound dressings revealed that during 40 h, the electrospun samples had variable water absorption between 0 and 0.25%. The results of the curcumin release test over one week showed that the nanofibers with PLA+Cur+2%AgNPs exhibited the lowest release rate, while those with PLA+Cur+3%AgNPs showed the highest release. The assessment of mechanical properties revealed that the tensile strength of nanofibers increased by adding curcumin to polylactic acid, while the addition of a high content of AgNPs led to a decrease in tensile strength. Also, the PLA+Cur wound dressing demonstrated 84.06% and the one with PLA+Cur+3%AgNPs exhibited 99.12% antibacterial properties. The cell culture test demonstrated that the incorporation of curcumin and AgNPs, both the growth and proliferation, as well as the adhesion on the nanofibrous wound dressing, increased well. Thus, the

PLA+Cur+1%AgNPs nanofibrous scaffold, as a multipurpose dressing, presented considerable promise for wound healing and burn treatment.

Keywords: Nanofibrous, Polylactic acid, Curcumin, Silver nanoparticles, Wound dressing, Electrospinning.

1. Introduction

The problems of bacterial infections causing chronic wounds threaten the lives of numerous patients and therefore require specialized treatment and care methods. Meanwhile, the improper use of antibiotics has resulted in a significant increase in bacterial resistance [1, 2]. One approach to overcome this problem involves the localized release of the drug and the utilization of wound dressings with antibacterial properties. Although the use of synthetic polymer scaffolds is prevalent in the medical field due to their biocompatibility and biodegradability, these materials usually do not have inherent antimicrobial properties. Nevertheless, they can be used as carriers for drugs or be combined with other antimicrobial substances [3-5]. Fibrous scaffolds based on polylactic acid offer valuable advantages for wound healing and tissue regeneration. Their unique features, such as high porosity, high surface area to volume, surface morphology, and fibrous diameter, which can be controlled by adjusting the parameters of the electrospinning process, make them suitable for these applications [2, 6]. On the other hand, in the electrospinning process, incorporating various suitable materials and making a nanocomposite scaffold can overcome the limitations of synthetic polymers. This enables the scaffold to acquire unique properties, such as antibacterial features and drug delivery capabilities [7-9]. It is important to keep in mind that different variables during electrospinning processing affect the shape of fibrous, comprising their diameter, porosity, and surface structure. These variables involve the operating distance in the electrospinning device, spinning voltage, solution feeding rate, needle inner size, and suspension viscosity, which is governed by the polymer content and additives [9-11]. It has been found that as the solution jet travels from the needle to the metal collector, it may split into multiple jets, resulting in a uniformity of fibrous diameters [9-11]. Regarding the additive for PLA-based nanofibrous scaffolds, curcumin has been extensively employed to cure several illnesses and skin conditions [10]. Curcumin possesses noteworthy properties in wound healing due to its anti-inflammatory, antioxidant, anti-cancer, anti-coagulant, and anti-infective effects, which accelerate the natural wound healing process at different stages. Recent studies indicate that curcumin can

reduce the body's natural response to skin wounds, including inflammation and oxidation [11]. Studies have been conducted on the use of curcumin in combination with other polymers. The results demonstrate the outstanding biocompatibility of curcumin loaded in nanofibers for wound applications. Curcumin has the potential to induce cell proliferation and enhance the process of wound healing [11, 12]. Curcumin is useful in eliminating reactive oxygen species, which promotes the accumulation of collagen in the development of granulation tissue and quickens the closure of wounds, both of which hasten the course of healing [12, 13]. Since curcumin exhibits low solubility in water compared to polymer, processing it in order to render it accessible for applications necessitates the use of micro and/or nanomaterials [14, 15]. Also, according to the research, PLA nanofibers loaded with curcumin exhibit favorable therapeutic properties. PLA and poly lactic-co-glycolic acid (PLGA) nanofibers containing curcumin are suitable materials for drug delivery, demonstrating effectiveness against cancer in laboratory conditions [16]. Accordingly, adding AgNPs to curcumin may substantially boost its antibacterial performance towards both Gram-positive and Gram-negative bacteria [17, 18]. In another study, the antimicrobial properties of AgNPs were reported in relation to the growth of *E. coli* cultured on agar plates. The results obtained show that the inhibition is dependent on both the concentration of AgNPs and the initial number of cells used in the experiments [19]. Silver has a strong antibacterial effect by causing damage to the DNA in the microorganism cell [20]. In addition to antibacterial activity, research has concentrated on exploring the therapeutic properties of silver and its nanoparticles, which has resulted in the development of various wound dressings with enhanced antibacterial effects. It has been demonstrated that activated carbon fibers containing silver increases the proliferation of fibroblasts in the skin. It has also been proven that prolonged exposure of epithelial cells to silver nanoparticles stimulates them to secrete TGF-β [17, 18, 20]. AgNPs solution was used for treating superficial wounds, revealing that this treatment accelerates wound healing in a shorter time and with better skin regeneration [21, 22]. Another study aimed to investigate the wound-healing potential of collagen nanofibrous dressings containing silver nanoparticles. The in vivo study revealed an accelerated speed of wound healing of composite nanofibrous wound dressings compared to non-composite collagen nanofibrous. Ulcerological analysis showed an acceleration in re-epithelialization, collagen production, and improved wound contraction with AgNPs composite collagen nanofibrous [22-24].

Considering the limitations of synthetic polymers and, on the other hand, as mentioned, acknowledging the special characteristics of curcumin and silver nanoparticles, the current research focused on developing a multi-component nanofibrous wound dressing with the electrospinning technique. The dressing was created from a combined solution of polylactic acid, curcumin, and silver nanoparticles with different concentrations, intended for burn treatment and wound dressing applications. The fabricated nanofibrous wound dressings were assessed through various methods, including Fourier transform infrared spectroscopy (FTIR), scanning electron microscopy, water absorption testing, drug release rate measurement, bacterial assays, mechanical properties testing, and cell culture analysis to observe morphological, moisture, and antibacterial behavior.

2. Materials and methods

2.1. Materials and electrospinning process

The electrospinning solution was prepared by polylactic acid $(C_3H_4O_2)_n$ granules with a nominal size of 3 mm and a molecular weight of 60000 g/mol from SIGMA, curcumin ($C_{21}H_{20}O_6$, MW = 368.38, Xiya Reagent Co., Ltd., China) with a molecular weight of 368.38 g/mol from Merck, and silver nanoparticles (AgNPs, 99.99% purity) with a particle size of 20 nm from US Research Nanomaterials, Inc. In addition, dichloromethane (DCM, Merck) and dimethylformamide (DMF, Merck) were employed as solvents.

In order to prepare a solution of 15 wt% PLA (Sample No. 1), 1.5 gr of PLA, previously dried in an oven at 70°C for 2 h, were thoroughly mixed using an electric stirrer with 7 mL of dichloromethane and 3 mL of dimethylformamide for 40 min. In the next step, sample solution 2, PLA+Cur was prepared by initially preparing two distinct solutions. The first solution involved dissolving 1.5 gr of dried polylactic acid in 7 mL of dichloromethane and the second solution contained 2.2 gr of curcumin dissolved in 3 mL of dimethylformamide solvent. Following preparation, these two solutions were combined and placed on the stirrer again for further mixing. Ultimately, to produce fibrous PLA+Cur+1 wt.% AgNPs (containing 0.015 gr Ag; sample 3), PLA+Cur+2 wt.% AgNPs (containing 0.03 gr Ag; sample 4), and PLA+Cur+3 wt.% AgNPs (containing 0.045 gr Ag; sample 5), 1wt.% Ag (0.015 gr Ag), 2 wt.% Ag (0.03 gr Ag), and 3 wt.% Ag (0.045 gr Ag) were added to the previously prepared PLA+Cur solution. To ensure complete suspension of the nanoparticles, each solution was placed on a stirrer for 2 h (Scheme. 1).

For the electrospinning process, the prepared solutions were transferred into 5 ml syringes with a G22 needle. Subsequently, the tip of the syringe needle and an aluminum foil as a collector were positioned at a distance of 15 cm from each other. The voltage difference between the tip of the needle and the aluminum foil was adjusted to 20 kV, and the flow rate was set to 0.5 mL/h. Electrospinning was carried out for 4 hours to achieve optimal results, ensuring the production of uniform fibers without bead formation by observing through a light microscope. During electrospinning, the solvents evaporated, leaving only the fibers adhered to the aluminum foil.

Scheme. 1.

2.2. Characterization

To identify functional groups and bonds formed in the electrospun samples, infrared spectroscopic analysis (PerkinElmer, USA) was employed within the wavelength range of 400-4000 cm^{-1}. The surface morphology of the electrospun samples was examined utilizing a scanning electron microscope (ESEM, Quanta 200, FEI). The mean and distribution of fibrous diameter was determined by measuring fibrous diameter in SEM micrographs with image processing software (Image J, National Institutes of Health, USA). Also, to ascertain the type and percentage of elements, Energy Dispersive X-ray Spectroscopy (EDAX analysis) was utilized. The mechanical behavior of the electrospun samples was measured using a universal tensile testing machine (SANTAM-20, Iran). Each tensile test was performed at room temperature using a crosshead speed of 5 mm/min. The findings were presented in the form of stress-strain curves.

The water absorption capability of the electrospun samples was tested at intervals of 1, 2, 3, 17, and 40 h. For this purpose, pieces of the sample with dimensions of 1×1 cm^2 were prepared and weighed using a scale with an accuracy of 0.0001 gr. The prepared samples were inserted in falcon tubes containing 5 cc of distilled water. Then, the falcon tubes were placed in an incubator with a temperature of 37 ^{o}C. After the specified period, the samples were taken out from the incubator, their surface water was filtered through filter paper, and their weight was re-measured using a scale. At the end, the amount of water absorption or swelling rate (S_w) of the samples was calculated according to Eq. 1.

$$S_w = (W_1 - W_0)/W_0 \quad (1)$$

where W_0 is the dry weight of the sample and W_1 is the weight of the wet sample after absorbing water.

2.3. Drug release test

For the release test, electrospun samples containing curcumin in dimensions of 1×1 cm^2 were used. The electrospun samples were placed in Falcon tubes containing 5 cc of distilled water and phosphate-buffered saline, supplemented by Tween 80 (Polysorbate 80, polyoxyethylene sorbitan monooleate), at concentrations of 5 to 100 ppm (via dilution). Then, the Falcon tubes were placed in the refrigerator for durations of 4 to 168 h. After each time interval, the samples were taken out of the solution and transferred into the same amount of solution in a new falcon tube, ready for the subsequent time interval. The preceding solutions were stored in the refrigerator. It should be noted that initially, the maximum absorption wavelength for curcumin was determined to establish a calibration line. Finally, their absorption at the maximum absorption wavelength (423 nm) was determined using the equation derived from the curcumin drug calibration line. The amount of light absorption of different samples was measured using ultraviolet spectrophotometry (UV-Vis, LAMBDA 750, PerkinElmer). Curcumin release was evaluated for each sample, and a cumulative graph was plotted against time. Thus, the concentration graph was generated according to the absorption rate of curcumin in distilled water and phosphate-buffered saline.

2.4. Antibacterial test

In this study, *Staphylococcus aureus* was employed to evaluate antibacterial activity. The antibacterial activity of the sample was assessed using the colony-forming unit (CFU) method. The samples were sterilized with 70% ethanol and a physiological solution. Subsequently, a bacterial suspension was prepared according to the McFarland standard, and its optical density (OD) was measured at a wavelength of 630 nm. Then, 1000 microliters of the bacterial suspension were poured on the blank samples, followed by an incubation period of 24 h at 37±1 °C. After the mentioned period, dilution was carried out at a ratio of 1:10, and the diluted bacteria were plated onto a nutrient agar culture medium. The plates were then incubated for 18 h at 37 ± 1 °C. The average number of colonies after incubation was determined using the ImageJ program, and the antibacterial efficacy of the sample was reported as a percentage according to Eq. 2.

$$R(\%)=(N_A-N_B)/N_A \times 100 \quad (2)$$

where R (%) represents the antibacterial effectiveness of the sample in percentage, N_A is the number of colonies in the sample before exposure to the antibacterial agent, and N_B is the number of colonies in the sample after exposure to the antibacterial agent.

2.5. Cytotoxicity assay

In this assay, L929 cells (NCBI C161) sourced from the cell bank of the Pasteur Institute of Iran were utilized. Culturing the cell was performed in a humidified environment with 5% CO_2 at 37 °C, and the culture media were replenished every 48 h. When the cells reached 80 to 90% confluency, they were detached using 0.25% trypsin/EDTA and then sub-cultured at a density of 10^5 cells per cm^2 in a 100 mm petri dish. Cells from the 3rd-6th passage of L929 cells were utilized for the tests. All cell assay experiments were performed in triplicate for every sample type at every time point, and the experiments were repeated at least once. The cell viability assay was conducted employing an indirect contact technique. The L929 cells were seeded in a 96-well plate at a density of 2×10^4 cells per mL with 100 µL of suspension for every well and incubated for 24 h to allow attachment. Following this step, the culture medium was removed and 100 microliters of MTT (dimethyl thiazyl diphenyl tetrazolium bromide test, MTT, Sigma, USA) solution, with a concentration of 0.5 mg/ml, was added to each well and placed in an incubator for 4 h. After the 4-h incubation period, the solution was removed from the cells, and isopropanol was added to dissolve the purple formazan crystals. To facilitate better dissolution of the MTT sediment, the plate was placed on a shaker for 15 min. Then, the concentration of the substance dissolved in isopropanol was determined using an ElizaReader device (BioTek ELx808, USA) at a wavelength of 570 nm. The well with more cells exhibits a higher optical density (OD) compared to the well with fewer cells, according to Ref. [25].

2.6. Statistical analysis

The mean value ± standard deviation was used to display the data analysis. Software designated GraphPad Prism (V.8) was used to perform statistical analysis. When $*p < 0.05$ and $**p < 0.01$, the data differences were considered statistically significant.

3. Results and discussion

3.1. FTIR spectra

The FTIR spectra for PLA, PLA+Cur, PLA+Cur+xAgNPs nanofibrous samples are shown in Figure 1. In the spectrum of the polylactic acid-curcumin-AgNPs sample, the broad peak at wavenumber 3463 cm^{-1} is attributed to either the stretching vibration of O–H in the curcumin structure or to the adsorbed water [26]. The peaks at wavenumbers of 2929 cm^{-1} and 2942 cm^{-1}, respectively, are related to the asymmetric and symmetrical stretching vibrations of C–H in the

aliphatic structures of PLA and curcumin [27]. Also, the peaks observed at wavenumbers of 1756 cm^{-1} and 1585 cm^{-1}, respectively, correspond to the stretching vibrations of C=O bonds in the carbonyl and carboxyl structures in PLA and curcumin, and the stretching vibration of C=C in the aromatic rings of curcumin [28]. In addition, the peaks at wavenumbers of 1452 cm^{-1}, 1365 cm^{-1}, and 1186 cm^{-1} are attributed to the bending vibrations of C–H in methyl and methylene groups, and the stretching vibration of the C–OH bond in the curcumin structure, respectively [29]. Furthermore, the peaks detected at wave numbers 1090 cm^{-1} and 888 cm^{-1}, respectively, are related to C–O–C stretching vibration in PLA and twisting vibration of C–H in curcumin and PLA structure [28-30]. Finally, after introducing AgNPs, a shift of the chitosan (CS) peaks at 3356 cm^{-1} was noticed, which is explained by the interaction of the reduced Ag with CS. Additionally, the hydroxyl peak's strength was found to have decreased. Therefore, as indicated by the FTIR test results, the presence of PLA, curcumin, and AgNPs in these composites is evident.

Fig. 1.

3.2. Microscopic evaluation

Figure 2 shows the SEM images of PLA, PLA+Cur, and PLA+Cur+xAgNPs nanofibrous samples. As can be seen from Figure 2a, the PLA electrospun nanofibrous scaffold has no beads, appropriate morphology, and a uniform diameter distribution, with an average diameter of 218 nm, along with uniform void space. However, the aforementioned parameters are constants in the present study. As seen in Figure 2b, the PLA+Cur electrospun nanofibrous scaffold has no beads, uniform void space, and an average fibrous diameter of 240 nm. It is worth mentioning that the addition of curcumin results in a color change in the fibrous, which is observable to the naked eye; the lighter, somewhat yellow coloration observed on the electrospun wound dressing indicates the presence of curcumin, which is effectively dispersed among the fibrous [31-33]. As evident from the comparison to PLA nanofibers, the presence of curcumin results in fibers that are more uniform and continuous, with void spaces that also have a better fit. Additionally, there is no visible accumulation of curcumin on the surfaces. Hence, it is evident that increasing the amount of curcumin in PLA substantially reduces the diameter of the nanofibers and improves the uniformity of the fibers. An interconnected porous structure, formed by loosely stacked nanofibers, was observed. In Figures 2c-e, respectively, SEM images of PLA, PLA+Cur, and PLA+Cur+xAgNPs nanofibrous samples can be seen. In these images, the presence of AgNPs is clearly discernible,

and the fibers exhibit uniform distribution, appropriate diameter, and spacing. The average fibrous diameters for electrospun samples 3, 4, and 5 are 140, 135, and 117 nm, respectively, indicating a decrease in fibrous diameter due to the presence of AgNPs. The smooth fibrous with regular morphology and relatively narrow dimensional distribution, which were smaller than pure PLA fibrous, can be due to the increase in conductivity of the solution resulting from the addition of AgNPs [33]. AgNPs with high electrical conductivity are being incorporated, and this dramatically raises the conductivity of the polymer solution, which escalates electric charges and reduces the diameter of the polymer fibers. In this context, elevating the solution's conductivity could yield a significantly more homogenous fibers combined with a decrease in the fibrous diameter [18]. To confirm the presence of AgNPs, EDX analysis was conducted on PLA+Cur+3%AgNPs nanofibrous sample. The result of this test is presented in Figure 2f. As evident from this spectrum, the strong peak confirms the presence of silver in this electrospun sample.

Fig. 2.

3.3. Water absorption evaluation

Figure 3 displays the bar graph illustrating the water absorption of PLA, PLA+Cur, and PLA+Cur+xAgNPs nanofibrous samples at various soaking times. As can be seen, the water absorption of all five wound dressing samples varies from 0.0004 to 0.0045 gr samples over the 40 h testing period. In the initial sample containing only PLA polymer, the water absorption varied over time, so that at certain intervals, there was either a negligible increase in weight or no change at all, indicating its hydrophobic nature. S. Krishnamohan et al. [34] displayed that the water absorption of pure PLA film varied from 0% to 0.02% during a 10-day experiment. Furthermore, the composite exhibited varying degrees of water absorption, with fluctuations occurring unevenly during the experiment. The utilization of PLA as a hydrophobic component was confirmed by test results, indicating its substantial resistance to water. Surface modification of PLA with plasma can enhance the hydrophilicity of the polymer. In the PLA+Cur sample, a wound dressing containing curcumin, the fluctuation in water absorption was more pronounced, likely attributable to the hydrophobic nature of curcumin, with a significant reduction in water absorption with time extension. In the PLA+Cur+1%AgNPs sample, which is a combination of fibers with curcumin and AgNPs, there was a very small increase in water absorption, rising from 0.0011 to 0.0036 gr. Research has shown that integrating curcumin into a nanoparticle-polymer composite could offer an alternative and easier approach to enhancing the solubility of curcumin in the water while

diminishing its hydrophobic characteristics [35]. In the PLA+Cur+2%AgNPs sample, the augmentation of AgNPs intensified hydrophobicity, consequently resulting in a decrease in water absorption once more. Regarding the PLA+Cur+3%AgNPs nanofibrous, with a further addition of AgNPs, water absorption has decreased. As evident from the graph, the addition of curcumin led to a reduction in water absorption, attributed to its inherent hydrophobic nature. Subsequently, with the incorporation of AgNPs, further fluctuations in water absorption occurred, arising from the presence of AgNPs within the polymer matrix and their hydrophobic properties. In this context, significant differences between the water absorption percentages of PLA+Cur+1%AgNPs and PLA+Cur nanofibers were observed ($p < 0.05$). In general, it is observed that as the quantity of AgNPs increases, water absorption decreases further.

Fig. 3.

3.4. Drug release behavior

Figure 4 displays the curves illustrating the changes in released curcumin for various samples during the immersion time. According to this diagram, the release of curcumin was notably high within the first 4 h in all the samples. However, with the passage of time, there was a tendency for the released curcumin to diminish. As indicated by this diagram, the strongest release of curcumin within the first 4 h was related to PLA+Cur+1%AgNPs, followed by samples PLA+Cur, and nanofibrous containing 2 and 3% AgNPs. Furthermore, according to this figure, for PLA+Cur+3%AgNPs sample, between approximately 145 and 168 h, there was an increase in the release of curcumin again. Indeed, in the PLA+Cur+3%AgNPs sample, the lack of strong release during the initial immersion periods suggests that the drug was stored within the carrier. Accordingly, this stored drug was subsequently released for longer periods of time. The structure of nanofibers facilitates a sustained and controlled release of curcumin over time. Due to the low degradation rate of PLA, the release mechanism often involves the diffusion of curcumin through the PLA matrix. However, there was no significant difference between curcumin release for PLA+Cur and PLA+Cur+3%AgNPs nanofibrous samples between 15 and 168 h ($p > 0.05$). Hemostasis, inflammation, growth, and reconstruction are the four interaction phases of the wound repair procedure, during which time fresh skin tissue may develop. Even while wounds recover in an orderly fashion, chronic wounds might result in an unfinished, drawn-out process of recovery that does not restore integrity. Under these circumstances, there is an overabundance of oxidative

stress, which fuels more oxidative stress and prolongs inflammation. Consequently, curcumin's short-term release may aid in the repair of wounds due to its anti-inflammatory and antioxidant characteristics. A continuous release of curcumin (81.5%) from CS-polyethylene glycol NPs was reported. The histologic examination demonstrated increased collagen and granulation tissue production, which hastens the repair of wounds [25].

On the other hand, the stability of nanoparticles is an important parameter for both biological applications and storage. The evolution of curcumin in chitosan /polyvinyl alcohol/sodium alginate (CS/PVA/SA) hydrogels with various combinations of Ag_2O/SiO_2 nanoparticles was investigated. It was demonstrated that in hydrogels without NPs, the evolution of curcumin occurred rapidly, reaching its peak within 16 h, and after that, no significant further evolution of curcumin was observed. By adding and increasing the percentage of nanoparticles in the hydrogel, the release of curcumin became slow, continuous, and balanced [36]. The porosity of the NPs and the bonds that occurred between curcumin and the nanoparticles as the hydrogel's NPs amount grew were responsible for the slow, steady, and balanced synthesis of curcumin. Conversely, when the proportion of NPs rose, these bonds became more prevalent, which decreased the amount of drug release. Additionally, a number of curcumin molecules became trapped in the porosity of hydrogels and NPs, which resulted in their partial release from the hydrogel structure.

Fig. 4.

3.5. Mechanical behavior

The stress-strain curves for different samples are presented in Figure 5. As evident, the addition of curcumin to PLA has resulted in an increase in nanofibrous tensile strength, which subsequently decreases with higher percentages of AgNPs. The increase in tensile strength upon adding curcumin to polylactic acid indicates good miscibility between these two substances, which implies that there is a significant interaction between curcumin and PLA. In a study, it was observed that in the first step, the addition of curcumin resulted in the formation of a random "beads fibrous" feature in the fibrous; however, no chemical reaction occurs between curcumin and PLA based on the FTIR results. Several studies have considered such an irregular formation. Such an irregular formation characterized by the "beads fibrous" feature may be due to the low solubility of curcumin, leading to accumulation during preparation, and generally, the tensile modulus and fibrous strength increase with increased molecular orientation, average molecular weight, and crystallization. The strength and modulus of PLA decrease with an increase in the

amount of curcumin in the matrix, so that when curcumin is added at 5% of the weight, the strength and modulus decrease by 35% and 37%, respectively [37]. On the other hand, nanoparticles act as stabilizers by linking polymer chains and preventing them from breaking. In a study, to be able to look into the impact of the weight fraction of nanoparticles, the distribution of atomic strains was compared between pristine nanofibers and those loaded with AgNPs in two concentrations (3.9% and 5.8%). Although the elastic performance of nanofibers loaded with 3.9% AgNPs is relatively greater compared to the sample containing 5.8% AgNPs, potentially owing to local strain near the added NPs, the enhancement in fracture resistance is significantly greater with the 5.8% sample. It's worth noting that the outcomes likewise depend on the placement at which the nanoparticles are released. Here, the nanoparticles are located in the middle of the doped nanofibers, which does not play a favorable role as the polymer chains begin to crack on one side. Nanoparticles restrict the motion of polymer chains and lessen the local atomic strain inside the nanofibrous [38]. The interactions between silver nanoparticles and the polymer matrix (PLA) can influence the molecular arrangement and chain entanglement of the polymer. Adverse interactions, such as reduced polymer chain mobility or cross-linking, may lead to a decrease in the overall mechanical strength of the nanofibrous. Interactions between curcumin and silver nanoparticles may influence their dispersion and behavior within the nanofibrous.

In another study, a set of keratin/poly(vinyl alcohol)/poly(ethylene oxide) nanofibers with different contents of AgNPs was prepared using electrospinning. Their characteristics were examined, and their outcome revealed that at a concentration of 1.2% silver nanoparticles, both the tensile strength and elongation at break reached their maximum values. The tensile properties of the composite nanofibers made with varying AgNP levels exhibited that as AgNP content rose, the tensile strength first elevated and then declined. The frequent breakdown and compaction of the nanofibers caused by the aggregation of AgNPs was likely responsible for the loss in tensile characteristics detected when the content of AgNPs exceeded 1.2%. It has been shown that AgNPs reduce the mechanical characteristics of composite fibrous [39].

However, the encapsulation of a high amount of AgNPs tends to agglomerate, forming clusters. Such clusters can serve as stress concentrators, resulting in a decrease in mechanical strength. Agglomeration may also disrupt the uniform distribution of nanoparticles within the nanofibers, thereby affecting their structural integrity. However, the strength and elastic modulus of the AgNPs-encapsulated PLA+Cur nanofibers were significantly altered by AgNPs. Overall, the

addition of 1 wt% AgNPs into PLA+Cur has a less significant effect on the strength and elongation at break, while the incorporation of 3 wt% AgNPs into nanofibers leads to a diminishment of both tensile strength and tensile strain. Due to their coarser structure and broad ranges in diameter, the electrospun nanofibers encapsulated with a high content of AgNPs are held accountable for this decrease in tensile strength. Accordingly, these findings demonstrate that the mechanical characteristics of PLA-based nanofibrous materials may fulfill dressing specifications for superior mechanical support and protection, which is crucial when applied to wound dressing utilization.

Fig. 5.

3.6. Antibacterial activity

Figures 6a-f show the antibacterial activity levels of PLA+Cur, PLA+Cur+1%AgNPs, and PLA+Cur+3%AgNPs samples relative to the blank sample against *S. aureus* bacteria. As evident from the figures, the presence of bacteria, depicted as white dots, has decreased, which indicates the destruction of the bacteria. According to the results of the CFU studies, the control specimen had a mean value of 849×10^6 CFU/mL, whereas the value of surviving *S. aureus* after 24 h of incubation was less than 108×10^6 CFU/mL following contact with the PLA+Cur specimen and 736×10^6 CFU/mL following contact with the PLA specimen. Specifically, as compared to other specimens, including the control specimen (795×10^6 CFU/mL), the PLA+Cur+Ag specimen showed the lowest bacterial activity (7×10^6 CFU/mL) against *S. aureus*.

All the nanofibrous samples exhibit higher antibacterial activity in comparison with the blank sample. Figure 6g illustrates the antimicrobial percentages that were obtained from the CFU outcomes. It is obvious from the graph that PLA+Cur+1%AgNPs have fewer bacteria than PLA+Cur, which has increased their antibacterial efficacy from 44.08% to 84.07%. When AgNPs were added, the antibacterial improvement elevated even more, reaching 99.12%. This suggests that the antibacterial decrease of the PLA-based nanofibrous is significantly impacted by the co-encapsulation of curcumin and AgNPs. Furthermore, PLA+Cur with an elevated AgNP concentration can release a bigger concentration of silver ions, which is mostly responsible for the increase in antibacterial performance when the AgNP concentration is increased from 1 to 3 wt.%. In this context, significant differences between the bacterial inhibition percentages of PLA+Cur and PLA+Cur+3%AgNPs nanofibrous were observed ($p < 0.05$). The primary cause of the effective antibacterial performance of the PLA/curcumin composite films' was curcumin's antimicrobial effects. Curcumin's primary mechanism of action is the disruption of FtsZ activity,

a protein required for bacterial survival and cell division. Curcumin has the ability to attach itself to the FtsZ protein and impede the synthesis of FtsZ protofilaments, hence impeding the development of the Z-ring, the proliferation of bacteria, and the migration of cells. It is also known that curcumin increases the FtsZ protein's GTPase function [40].

Additionally, films encapsulated with curcumin were found to have a strong antibacterial action with a high inhibitory zone toward *S. aureus*. Other studies exhibited that curcumin may prevent the growth of different bacteria in a comparable manner despite differences in cell walls. This could be owing to the fact that the antibacterial performance was linked to an augmentation of cell permeability through the process of electrostatic binding with positively charged molecules in the film [41]. The antibacterial effects of curcumin and AgNPs have been confirmed in previous research. AgNPs possess a wide range of antimicrobial properties against both fungi and bacteria, including strains resistant to antibiotics. This is because Ag, an active ingredient, has an antibacterial action. First, sulfhydryl groups within the cell wall are rapidly bound by Ag ions, which leads to the malfunctioning of these components in a variety of enzymes that contribute to the creation of transmembrane energy and fluid transport. The production of adenosine triphosphate (ATP) is then inhibited. Then, by attaching to thiol groups in areas like cytochrome oxidase and NADH-succinate dehydrogenase, Ag ions obstruct the respiratory system of bacteria, halting bacterial respiration and adenosine triphosphate generation. Lastly, by disrupting hydrogen bonds between neighboring purines and pyrimidines, Ag ions can attach to nucleotide bases and intercalate with double-stranded DNA molecules, inhibiting DNA polymerases from reproducing them [42]. AgNPs' ability to penetrate bacteria and interfere with their metabolic processes amplifies their antibacterial efficacy. There are two possible ways that Ag ions could be released: (i) polymer degradation leading to the release of non-reduced Ag ions that were formerly complexed with polymers and (ii) water diffusing through the polymer matrix and releasing Ag^{+} from nanoparticles. This modest Ag ion level may effectively have bacteriostatic impacts on *S. aureus* in vitro [43].

Furthermore, the antibacterial performance of PLA+Cur+3%AgNPs nanofibrous was higher, which may have been caused by the complementary effects of curcumin and AgNPs. It is possible that the PLA+Cur+3%AgNPs nanofibrous superior inhibitory activities against *S. aureus* were caused by its distinct cell wall structure [41]. Due to their binding to the peptidoglycan layer of bacteria, curcumin and AgNPs have been linked to bacterial destruction of membranes. Curcumin

and AgNPs have an antibacterial effect mainly because they interfere with the bacteria's DNA, proteins, and replication of cells [44].

According to Alves et al., AgNPs may improve curcumin's antibacterial activity when combined to create curcumin-AgNPs nanocomposites. Consequently, the following might be used to characterize curcumin-AgNPs primary antibacterial mechanism: Curcumin serves as a capping and reducing agent for each AgNPs, and (ii) the nanocomposites of curcumin-AgNPs bond to the bacteria to generate Ag^+ ions [45, 46]. Ultimately, the generation of Ag^+ ions results in the production of reactive oxygen species, which destroy membranes, as well as bacterial lipases, which allow intracellular contents to seep out and eventually result in bacterial death.

Fig. 6.

3.7. Biocompatibility

All materials that are used to treat wounds have to be biocompatible; therefore, the cytotoxicity indicator is frequently used to assess how well a material satisfies this crucial need. SEM images of PLA, PLA+Cur, and PLA+Cur+xAgNPs nanofibrous samples after cell culture are presented in Figures 7a-e, respectively. As it is evident from Figure 7a, cells exhibited a spindle-like shape as they adhered to and spread across the PLA-based wound dressings, firmly anchoring themselves onto the nanofibrous scaffolds. Furthermore, Figures 7b-e reveal that the addition of curcumin and silver nanoparticles, respectively, led to increased cell expansion and more comprehensive coverage of the nanofibrous, so that in a higher percentage of nanoparticles, a significant portion of the nanofibrous surfaces became enveloped by cells, resulting in the formation of multiple layers of cells on the fibrous. The graph also showed there was no significant difference ($p > 0.05$) between cell survival of PLA nanofibrous samples without AgNPs and with a low amount of AgNPs (Fig. 7). However, there is a significant difference ($p < 0.05$) observed between PLA and PLA+Cur+3%AgNPs nanofibrous samples for cell viability. In a comparable manner, Zhaonan Li et al. [58] demonstrated that, as compared to the PLA and PLA-4%AgNPs samples, the viable cells of CCC-HPF-1 cells on the PLA-6%AgNPs sample were the lowest numerous ($P < 0.0005$). The PLA-6%AgNPs and PLA samples exhibited significant differences, whereas the PLA-4 %AgNPs and PLA samples showed no differences, according to their live/dead test findings. Studies have revealed that Cur-AgNPs exhibit low cytotoxicity while promoting proliferation, migration, and collagen production in human dermal fibroblasts [47, 48].

Beyond the materials employed in scaffold construction, the morphology and structure of the fibers profoundly affect the behavior of the cells. The electrospinning method is a specialized technique

extensively utilized in wound healing applications, producing fibrous structures in the nano and micro ranges, as well as forming fibrous structures with a hollow structure, making it valuable in the realms of drug delivery and gene therapy. The size and positioning of the cavities on electrospun fibrous scaffolds are the key and influential factors in facilitating adhesion, proliferation, cell differentiation, and protein binding [47, 48]. It has been shown that electrospun nanofibers exhibit superior capabilities for cell growth, adhesion, and migration into the inner spaces of 3D porous scaffolds compared to many castable films [49]. The effects of curcumin and silver nanoparticles on cell growth and proliferation have also been documented by researchers in various studies. Previous experimental investigations on electrospun nanofibrous scaffolds incorporating silver nanoparticles have shown their significant role in facilitating cell absorption, proliferation, and growth [6, 11, 16, 50]. In the case of curcumin, while similar positive effects on cell adhesion and proliferation have been reported, its cytotoxic activity towards various cell types depends on both the dosage and the specific cell line [51, 52]. Furthermore, past research findings indicate that the combination of silver nanoparticles with other antibacterial agents has positive synergistic effects on cell behavior [53-58].

Fig. 7.

4. Conclusions

In the present study, PLA, PLA+Cur, PLA+Cur+1%AgNPs, PLA+Cur+2%AgNPs, and PLA+Cur+3%AgNPs nanofibrous scaffolds were fabricated using the electrospinning method for use as wound dressings. Investigations conducted using a scanning electron microscope revealed fibrous diameters ranging between 135 and 239 nm, with no beads and a uniform distribution in all nanofibrous samples. Due to the hydrophobic nature of PLA and curcumin, coupled with the characteristics of AgNPs, the results of the water absorption test showed values ranging between 0.0 and 0.25%, indicating negligible water absorption. The drug release test revealed that in the majority of samples, the release of curcumin exhibited a notable increase after 4 h, followed by relative stability over longer durations. The presence of curcumin enhances the tensile strength of the samples, while the presence of AgNPs decreases it. In the antibacterial evaluation, the presence of curcumin (84.06%) and the presence of AgNPs with curcumin (99.12%) exhibited effective bacteria destruction. In the MTT evaluation, the nanofibrous samples displayed no significant difference ($p > 0.05$) between cell survival of PLA nanofibrous samples without AgNPs and with a low amount of AgNPs (PLA+Cur+1%AgNPs) were observed. However, there is a significant

difference ($p < 0.05$) observed between PLA and PLA+Cur+3%AgNPs nanofibrous samples for cell viability. Taken together, our research's findings lend credence to the idea that encapsulation of Cur+AgNPs into PLA nanofibers is a viable approach for improving biocompatibility and antibacterial performance for use in burn treatment and wound healing.

References

[1] Chen S, Tian H, Mao J, Ma F, Zhang M, Chen F, et al. Preparation and application of chitosan-based medical electrospun nanofibers. International Journal of Biological Macromolecules. 2023;226: 410-22.

[2] Zhang M, Xu S, Wang R, Che Y, Han C, Feng W, et al. Electrospun nanofiber/hydrogel composite materials and their tissue engineering applications. Journal of Materials Science & Technology. 2023; 162:157-78.

[3] Deng S, Chen A, Chen W, Lai J, Pei Y, Wen J, et al. Fabrication of biodegradable and biocompatible functional polymers for anti-infection and augmenting wound repair. Polymers. 2023; 15(1): 120.

[4] Gul A, Gallus I, Tegginamath A, Maryska J, Yalcinkaya F. Electrospun antibacterial nanomaterials for wound dressings applications. Membranes. 2021; 11(12): 908.

[5] Parham S, Kharazi AZ, Bakhsheshi-Rad HR, Ghayour H, Ismail AF, Nur H, et al. Electrospun nano-fibers for biomedical and tissue engineering applications: A comprehensive review. Materials. 2020; 13(9): 2153.

[6] Hajikhani M, Emam-Djomeh Z, Askari G. Fabrication and characterization of mucoadhesive bioplastic patch via coaxial polylactic acid (PLA) based electrospun nanofibers with antimicrobial and wound healing application. International Journal of Biological Macromolecules. 2021;172: 143-53.

[7] El-Aassar MR, Ibrahim OM, Al-Oanzi ZH. Biotechnological applications of polymeric nanofiber platforms loaded with diverse bioactive materials. Polymers. 2021; 13(21): 3734.

[8] Kamaraj M, Moghimi N, Chen J, Morales R, Chen S, Khademhosseini A, et al. New dimensions of electrospun nanofiber material designs for biotechnological uses. Trends in Biotechnology. 2023.

[9] Syed MH, Khan MMR, Zahari MAKM, Beg MDH, Abdullah N. A review on current trends and future prospectives of electrospun biopolymeric nanofibers for biomedical applications. European Polymer Journal. 2023;197:112352.

[10] Pacheco KML, Torres BBM, Sanfelice RC, da Costa MM, Assis L, Marques RB, et al. Chitosan and chitosan/turmeric-based membranes for wound healing: Production, characterization and application. International Journal of Biological Macromolecules. 2023;253:127425.

[11] Perumal G, Pappuru S, Chakraborty D, Maya Nandkumar A, Chand DK, Doble M. Synthesis and characterization of curcumin loaded PLA—Hyperbranched polyglycerol electrospun blend for wound dressing applications. Materials Science and Engineering: C. 2017;76:1196-204.

[12] Akbik D, Ghadiri M, Chrzanowski W, Rohanizadeh R. Curcumin as a wound healing agent. Life Sciences. 2014;116(1):1-7.

[13] Sood A, Dev A, Das SS, Kim HJ, Kumar A, Thakur VK, et al. Curcumin-loaded alginate hydrogels for cancer therapy and wound healing applications: A review. International Journal of Biological Macromolecules. 2023;232:123283.

[14] Kumari M, Nanda DK. Potential of Curcumin nanoemulsion as antimicrobial and wound healing agent in burn wound infection. Burns. 2023;49(5):1003-16.

[15] Mohanty C, Sahoo SK. Curcumin and its topical formulations for wound healing applications. Drug Discovery Today. 2017;22(10):1582-92.
[16] Mitra S, Mateti T, Ramakrishna S, Laha A. A Review on Curcumin-Loaded Electrospun Nanofibers and their Application in Modern Medicine. JOM. 2022;74(9):3392-407.
[17] Choudhury H, Pandey M, Lim YQ, Low CY, Lee CT, Marilyn TCL, et al. Silver nanoparticles: Advanced and promising technology in diabetic wound therapy. Materials Science and Engineering: C. 2020; 112:110925.
[18] Bakhsheshi-Rad HR, Ismail AF, Aziz M, Akbari M, Hadisi Z, Khoshnava SM, et al. Co-incorporation of graphene oxide/silver nanoparticle into poly-L-lactic acid fibrous: A route toward the development of cytocompatible and antibacterial coating layer on magnesium implants. Materials Science and Engineering: C. 2020;111:110812.
[19] Khan MR, Urmi MA, Kamaraj C, Malafaia G, Ragavendran C, Rahman MM. Green synthesis of silver nanoparticles with its bioactivity, toxicity and environmental applications: A comprehensive literature review. Environmental Nanotechnology, Monitoring & Management. 2023;20:100872.
[20] Kumar M, Mahmood S, Chopra S, Bhatia A. Biopolymer based nanoparticles and their therapeutic potential in wound healing – A review. International Journal of Biological Macromolecules. 2024; 267:131335.
[21] Magdy G, Aboelkassim E, Abd Elhaleem SM, Belal F. A comprehensive review on silver nanoparticles: Synthesis approaches, characterization techniques, and recent pharmaceutical, environmental, and antimicrobial applications. Microchemical Journal. 2024;196:109615.
[22] Vishwanath R, Negi B. Conventional and green methods of synthesis of silver nanoparticles and their antimicrobial properties. Current Research in Green and Sustainable Chemistry. 2021;4: 100205.
[23] Fu X, Rehman U, Wei L, Chen Z-S, Abourehab MAS, Kesharwani P, et al. Silver-dendrimer nanocomposite as emerging therapeutics in anti-bacteria and beyond. Drug Resistance Updates. 2023;68:100935.
[24] Azizi-Lalabadi M, Garavand F, Jafari SM. Incorporation of silver nanoparticles into active antimicrobial nanocomposites: Release behavior, analyzing techniques, applications and safety issues. Advances in Colloid and Interface Science. 2021;293:102440.
[25] Safarpour F, Kharaziha M, Emadi R. Inspiring biomimetic system based on red blood cell membrane vesicles for effective curcumin loading and release. International Journal of Pharmaceutics. 2022;613:121419.
[26] Ghaee A, Bagheri-Khoulenjani S, Amir Afshar H, Bogheiri H. Biomimetic nanocomposite scaffolds based on surface modified PCL-nanofibers containing curcumin embedded in chitosan/gelatin for skin regeneration. Composites Part B: Engineering. 2019;177:107339.
[27] Li D, Jiang Y, Lv S, Liu X, Gu J, Chen Q, et al. Preparation of plasticized poly (lactic acid) and its influence on the properties of composite materials. PLOS ONE. 2018;13(3):e0193520.
[28] Arunraj TR, Sanoj Rejinold N, Ashwin Kumar N, Jayakumar R. Bio-responsive chitin-poly(l-lactic acid) composite nanogels for liver cancer. Colloids and Surfaces B: Biointerfaces. 2014;113:394-402.
[29] Roshanghias A, Sodeifian G, Javidparvar AA, Tarashi S. Construction of a novel polytetrafluoroe thylene-based sealant paste: The effect of polyvinyl butyral (PVB) and nano-alumina on the sealing performance and construction formulations. Results in Engineering. 2022;14:100460.
[30] Ramli RH, Fhong Soon C, Mohd Rus AZ. Synthesis of chitosan/alginate/silver nanoparticles hydrogel scaffold. MATEC Web Conf. 2016;78.

[31] Luz PP, e Silva MLA, Hinestroza JP. Curcumin-loaded biodegradable electrospun fibers: preparation, characterization, and differences in fiber morphology. International Journal of Polymer Analysis and Characterization. 2013;18(7):534-44.
[32] Ahmadi T, Monshi A, Mortazavi V, Fathi MH, Sharifi S, Kharaziha M, et al. Fabrication and characterization of polycaprolactone fumarate/gelatin-based nanocomposite incorporated with silicon and magnesium co-doped fluorapatite nanoparticles using electrospinning method. Materials Science and Engineering: C. 2020;106:110172.
[33] Bardania H, Mahmoudi R, Bagheri H, Salehpour Z, Fouani MH, Darabian B, et al. Facile preparation of a novel biogenic silver-loaded Nanofilm with intrinsic anti-bacterial and oxidant scavenging activities for wound healing. Scientific Reports. 2020;10(1):6129.
[34] Krishnamohan S, Anandaram H, Rathinam V, Kaliappan S, Sekar S, Patil PP, et al. Optimization of water absorption and mechanical and thermal behavior of polylactic acid/chitosan/titanium carbide. Advances in Materials Science and Engineering. 2022;2022: 5176584.
[35] Sarma R, Das M, Saikia L, Ramteke A, Saikia R. Conjugation of curcumin with Ag nanoparticle for improving its bioavailability and study of the bioimaging response. Nanosystems: Physics, Chemistry, Mathematics. 2021;12:528-35.
[36] Farazin A, Mohammadimehr M, Ghasemi AH, Naeimi H. Design, preparation, and characterization of CS/PVA/SA hydrogels modified with mesoporous Ag_2O/SiO_2 and curcumin nanoparticles for green, biocompatible, and antibacterial biopolymer film. RSC Advances. 2021;11(52):32775-91.
[37] Sharifah ISS, Qairol AAB, Azlina HN, Khairusshima MKN. Thermal, structural and mechanical properties of melt drawn Cur-loaded poly(lactic acid) fibers. Procedia Engineering. 2017;184:544-51.
[38] Izadi R, Trovalusci P, Fantuzzi N. A study on the effect of doping metallic nanoparticles on fracture properties of polylactic acid nanofibres via molecular dynamics simulation. Nanomaterials. 2023; 13(6): 989.
[39] He M, Chen M, Dou Y, Ding J, Yue H, Yin G, et al. Electrospun silver nanoparticles-embedded feather keratin/poly(vinyl alcohol)/poly(ethylene oxide) antibacterial composite nanofibers. Polymers. 2020; 12(2): 305.
[40] Song Y, Hu Q, Liu S, Wang Y, Zhang H, Chen J, et al. Electrospinning/3D printing drug-loaded antibacterial polycaprolactone nanofiber/sodium alginate-gelatin hydrogel bilayer scaffold for skin wound repair. International Journal of Biological Macromolecules. 2024:129705.
[41] Xie H, Ouyang K, Zhang L, Hu J, Huang S, Sun W, et al. Chitosan/rice hydrolysate/curcumin composite film: Effect of chitosan molecular weight. International Journal of Biological Macromolecules. 2022;210:53-62.
[42] Liu S, Zhao J, Ruan H, Wang W, Wu T, Cui W, et al. Antibacterial and anti-adhesion effects of the silver nanoparticles-loaded poly(l-lactide) fibrous membrane. Materials Science and Engineering: C. 2013;33(3):1176-82.
[43] Pishbin F, Mouriño V, Gilchrist JB, McComb DW, Kreppel S, Salih V, et al. Single-step electrochemical deposition of antimicrobial orthopaedic coatings based on a bioactive glass/chitosan/ nano-silver composite system. Acta Biomaterialia. 2013;9(7):7469-79.
[44] Akshaykranth A, Jayarambabu N, kumar A, Venkatappa Rao T, Kumar RR, Srinivasa Rao L. Novel nanocomposite polylactic acid films with Curcumin-ZnO: structural, thermal, optical and antibacterial properties. Current Research in Green and Sustainable Chemistry. 2022;5:100332.
[45] Wang Q, Liu S, Lu W, Zhang P. Fabrication of Curcumin@Ag Loaded Core/Shell Nanofiber Membrane and its Synergistic Antibacterial Properties. Frontiers in Chemistry. 2022;10.

[46] El-Kattan N, Emam AN, Mansour AS, Ibrahim MA, Abd El-Razik AB, Allam KAM, et al. Curcumin assisted green synthesis of silver and zinc oxide nanostructures and their antibacterial activity against some clinical pathogenic multi-drug resistant bacteria. RSC Advances. 2022; 12(28): 18022-38.
[47] Bhubhanil S, Talodthaisong C, Khongkow M, Namdee K, Wongchitrat P, Yingmema W, et al. Enhanced wound healing properties of guar gum/curcumin-stabilized silver nanoparticle hydrogels. Scientific Reports. 2021;11(1):21836.
[48] Madivoli ES, Kareru PG, Gichuki J, Elbagoury MM. Cellulose nanofibrils and silver nanoparticles enhances the mechanical and antimicrobial properties of polyvinyl alcohol nanocomposite film. Scientific Reports. 2022;12(1):19005.
[49] Liu C, Zhu Y, Lun X, Sheng H, Yan A. Effects of wound dressing based on the combination of silver @curcumin nanoparticles and electrospun chitosan nanofibers on wound healing. Bioengineered. 2022;13(2):4328-39.
[50] Alven S, Buyana B, Feketshane Z, Aderibigbe BA. Electrospun nanofibers/nanofibrous scaffolds loaded with silver nanoparticles as effective antibacterial wound dressing materials. Pharmaceutics. 2021; 13(7): 964.
[51] Akrami-Hasan-Kohal M, Tayebi L, Ghorbani M. Curcumin-loaded naturally-based nanofibers as active wound dressing mats: morphology, drug release, cell proliferation, and cell adhesion studies. New Journal of Chemistry. 2020;44(25):10343-51.
[52] Júnior AF, Ribeiro CA, Leyva ME, Marques PS, Soares CRJ, Alencar de Queiroz AA. Biophysical properties of electrospun chitosan-grafted poly(lactic acid) nanofibrous scaffolds loaded with chondroitin sulfate and silver nanoparticles. Journal of Biomaterials Applications. 2021;36(6): 1098-110.
[53] Hashemi S-S, Saadatjo Z, Mahmoudi R, Delaviz H, Bardania H, Rajabi S-S, et al. Preparation and evaluation of polycaprolactone/chitosan/Jaft biocompatible nanofibers as a burn wound dressing. Burns. 2022;48(7):1690-705.
[54] Li S, Liu Y, Huang Z, Kou Y, Hu A. Efficacy and safety of nano-silver dressings combined with recombinant human epidermal growth factor for deep second-degree burns: A meta-analysis. Burns. 2021;47(3):643-53.
[55] G. El Baassiri M, Dosh L, Haidar H, Gerges A, Baassiri S, Leone A, et al. Nerve growth factor and burn wound healing: Update of molecular interactions with skin cells. Burns. 2023;49(5):989-1002.
[56] Rangatchew F, Vester-Glowinski P, Rasmussen BS, Haastrup E, Munthe-Fog L, Talman M-L, et al. Mesenchymal stem cell therapy of acute thermal burns: A systematic review of the effect on inflammation and wound healing. Burns. 2021;47(2):270-94.
[57] Knoz M, Holoubek J, Lipový B, Faldyna M, Chaloupková R, Pavliňáková V, et al. Evaluation of viscoelastic parameters and photo-based assessment of newly developed dermal substitutes modified with thermostabilized fibroblast growth factor 2. Burns. 2024.
[58] Li Z, Jiao D, Zhang W, Ren K, Qiu L, Tian C, Li Y, Li J, Zhou X, Zhao Y, Han X. Antibacterial and antihyperplasia polylactic acid/silver nanoparticles nanofiber membrane-coated airway stent for tracheal stenosis. Colloids and Surfaces B: Biointerfaces. 2021;206:111949.

Caption of Figures

Scheme. 1. Schematic illustration of the synthesis of antibacterial PLA+Cur+AgNPs nanofibers

Fig. 1. FTIR analysis of the PLA, PLA+Cur, PLA+Cur+1%AgNPs, PLA+Cur+2%AgNPs, and PLA+Cur+3%AgNPs

Fig. 2. SEM images of electrospun fibers a) PLA, b) PLA+Cur, c) PLA+Cur+1%AgNPs, d) PLA+Cur+ 2%AgNPs and e) PLA+Cur+3%AgNPs, and (f) the EDX spectrum in conjunction with the SEM image pertaining to PLA+Cur+3%AgNPs nanofibers.

Fig. 3. Water absorption diagram of PLA, PLA+Cur, PLA+Cur+1%AgNPs, PLA+Cur+2% AgNPs, and PLA+Cur+3%AgNPs nanofibers

Fig. 4. The graph of changes in the concentration of curcumin released for PLA+Cur, PLA+Cur+1%AgNPs, PLA+Cur+2%AgNPs PLA+Cur+3%AgNPs nanofibers.

Fig. 5. Stress-strain curves of PLA, PLA+Cur, PLA+Cur+1%AgNPs, PLA+Cur+2%AgNPs, and PLA+Cur+3%AgNPs nanofibers.

Fig. 6. Images of the antibacterial activity of a, b) PLA+Cur versus the blank sample, and c, d) PLA+Cur+1%AgNPs versus the blank sample, and e, f) PLA+Cur+3%AgNPs versus the blank sample and g) bacterial inhibition against S. aureus bacteria regarding PLA+Cur+AgNPs nanofibers

Fig. 7. SEM images after cell culture of electrospun fibers a) PLA, b) PLA+Cur, c) PLA+Cur+1%AgNPs, d) PLA+Cur+2%AgNPs and e) PLA+Cur+3%AgNPs and f) cytotoxicity comparison graph of PLA, PLA+Cur, and PLA+Cur+AgNPs nanofibers

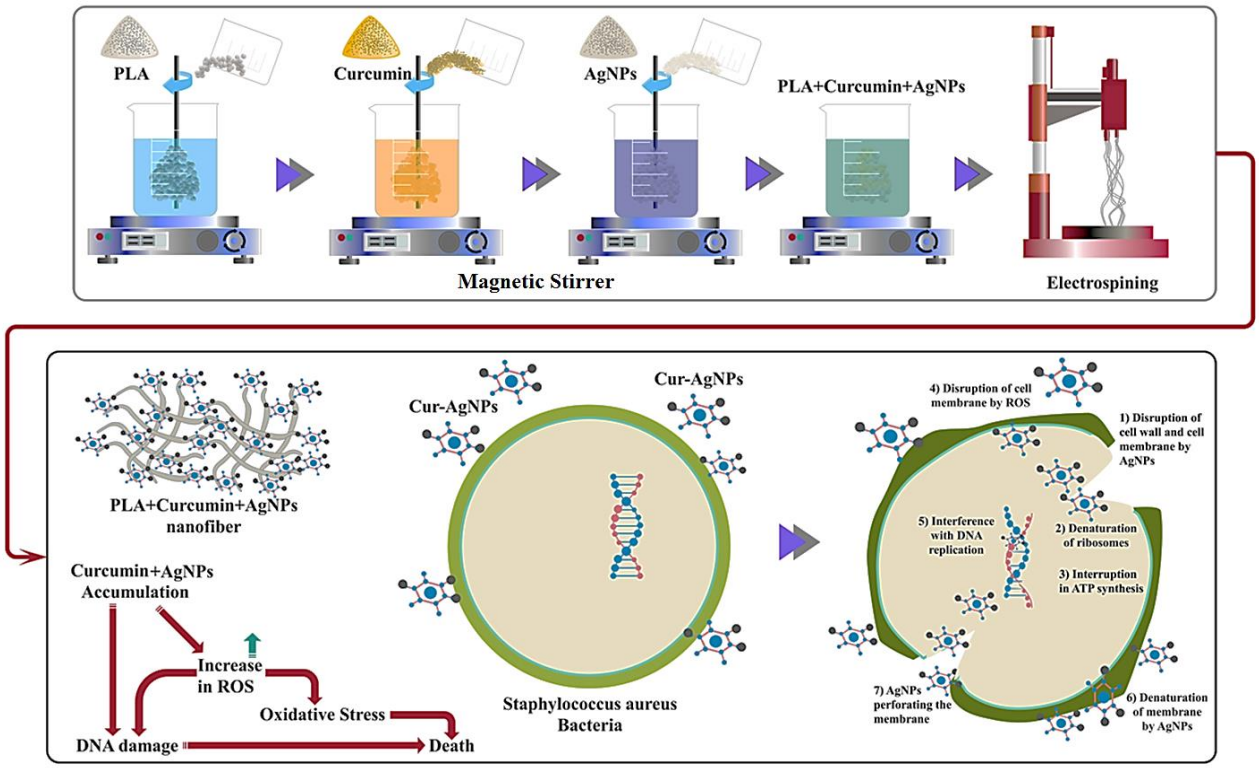

Scheme. 1. Schematic illustration of the synthesis of antibacterial PLA+Cur+AgNPs nanofibers

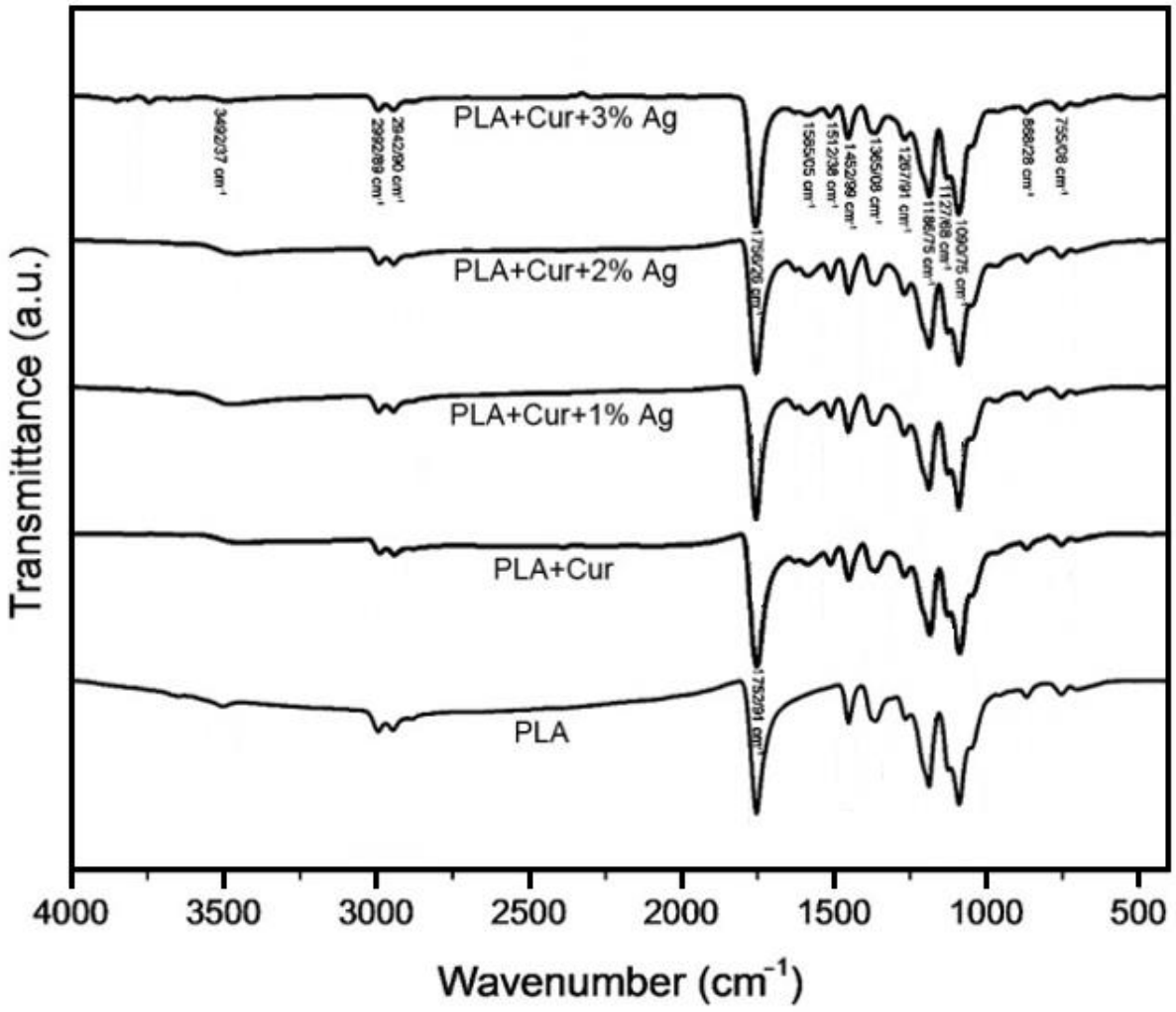

Fig. 1. FTIR analysis of the PLA, PLA+Cur, PLA+Cur+1%AgNPs, PLA+Cur+2%AgNPs, and PLA+Cur+ 3%AgNPs

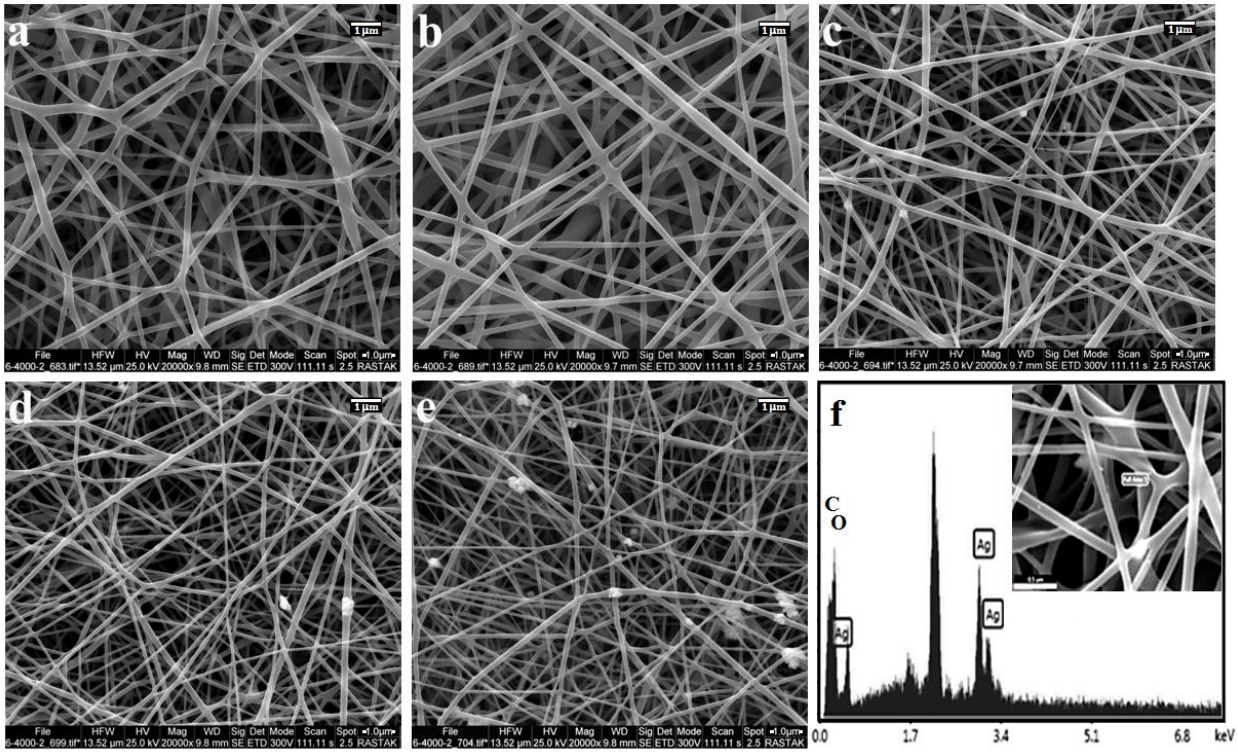

Fig. 2. SEM images of electrospun fibers a) PLA, b) PLA+Cur, c) PLA+Cur+1%AgNPs, d) PLA+Cur+ 2%AgNPs and e) PLA+Cur+3%AgNPs, and (f) the EDX spectrum in conjunction with the SEM image pertaining to PLA+Cur+3%AgNPs nanofibers.

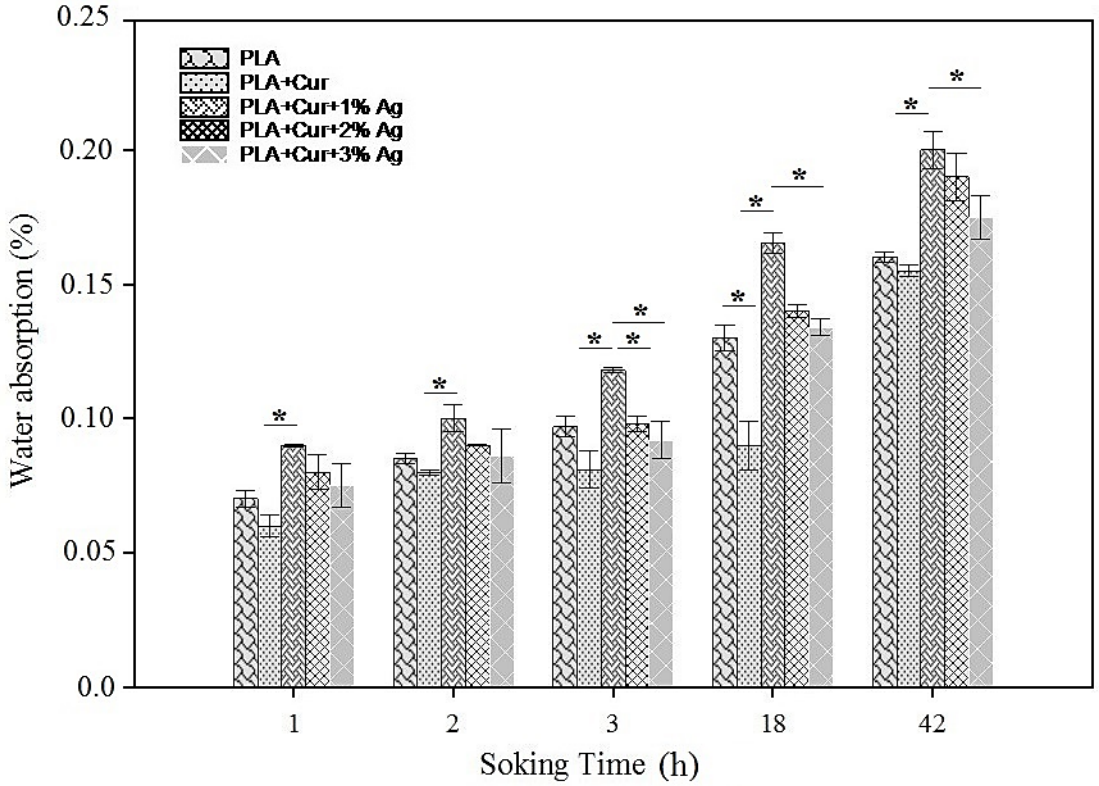

Fig. 3. Water absorption diagram of PLA, PLA+Cur, PLA+Cur+1%AgNPs, PLA+Cur+2% AgNPs, and PLA+Cur+3%AgNPs nanofibers

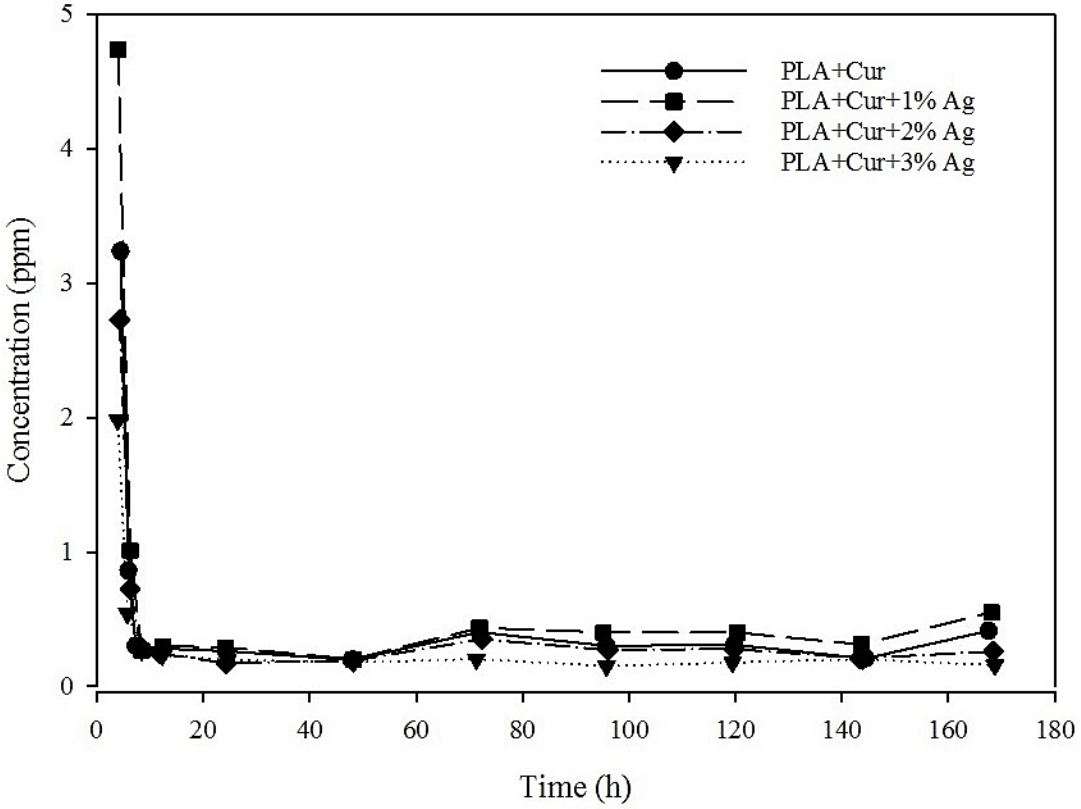

Fig. 4. The graph of changes in the concentration of curcumin released for PLA+Cur, PLA+Cur+1%AgNPs, PLA+Cur+2%AgNPs, and PLA+Cur+3%AgNPs nanofibers.

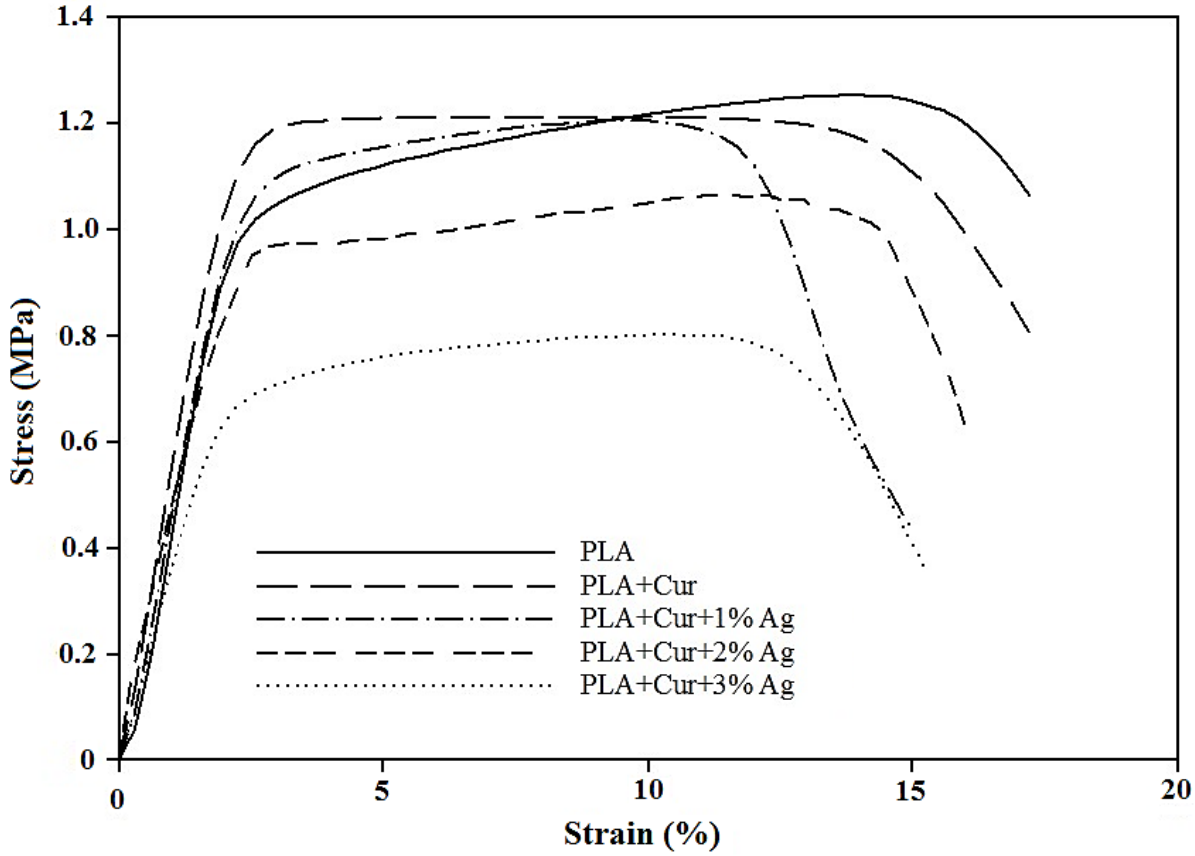

Fig. 5. Stress-strain curves of PLA, PLA+Cur, PLA+Cur+1%AgNPs, PLA+Cur+2%AgNPs, and PLA+Cur+3%AgNPs nanofibers.

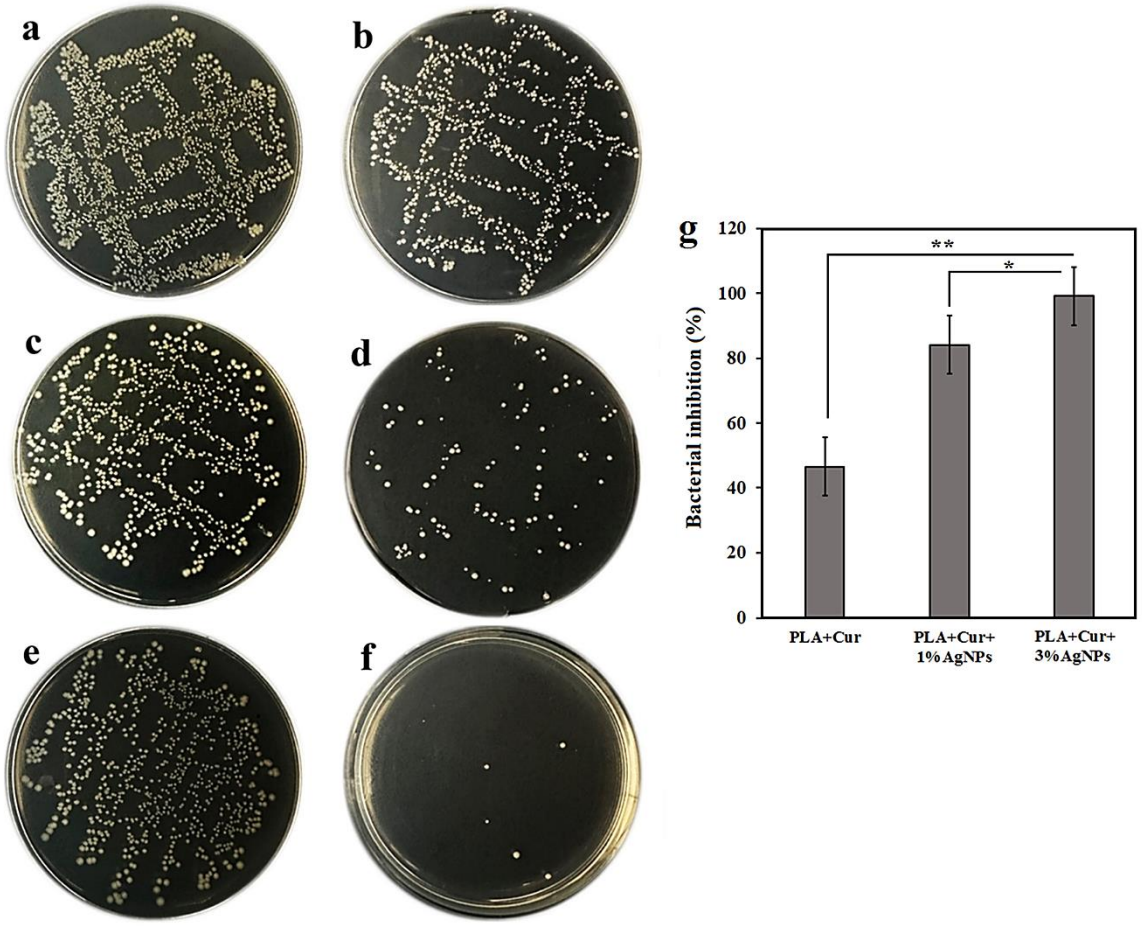

Fig. 6. Images of the antibacterial activity of a, b) PLA+Cur versus the blank sample, and c, d) PLA+Cur+1%AgNPs versus the blank sample, and e, f) PLA+Cur+3%AgNPs versus the blank sample and g) bacterial inhibition against S. aureus bacteria regarding PLA+Cur+AgNPs nanofibers

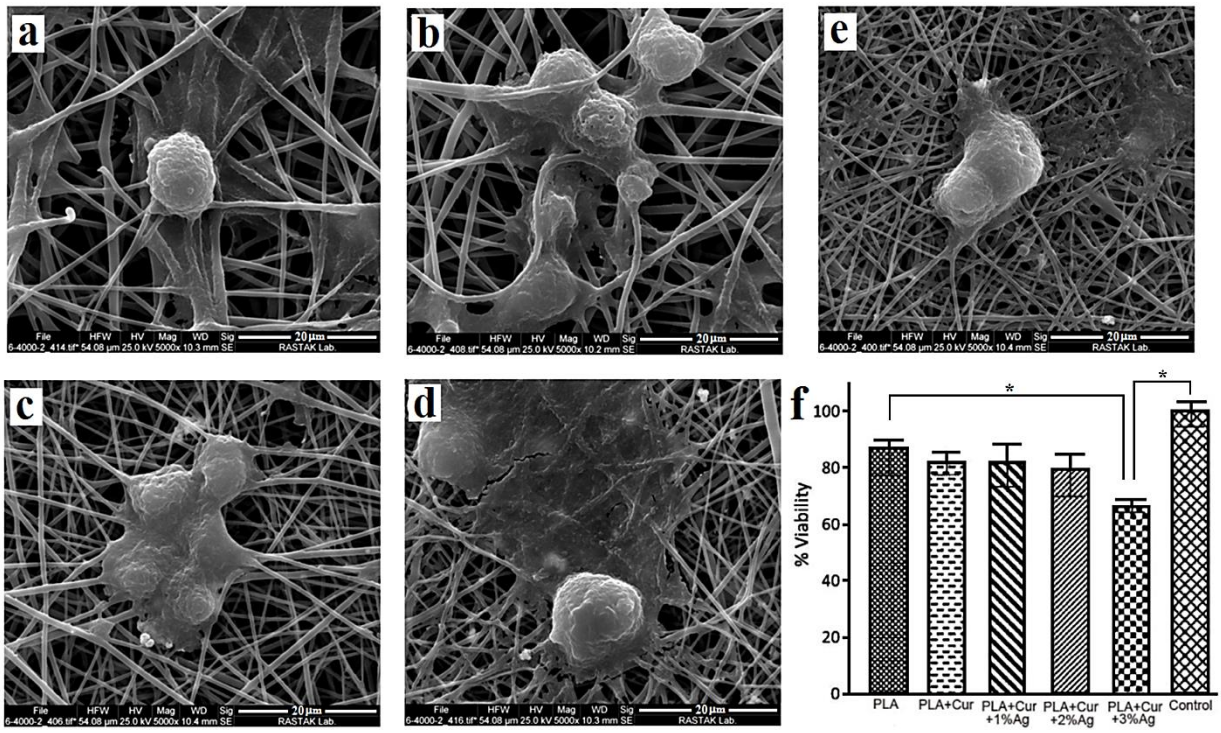

Fig. 7. SEM images after cell culture of electrospun fibers a) PLA, b) PLA+Cur, c) PLA+Cur+ 1% AgNPs, d) PLA+Cur+2%AgNPs and e) PLA+Cur+3%AgNPs and f) cytotoxicity comparison graph of PLA, PLA+Cur, and PLA+Cur+AgNPs nanofibers

Figure (300 dpi and editable format)

Click here to access/download;Figure (300 dpi and editable format);Scheme. 1-R2.tif

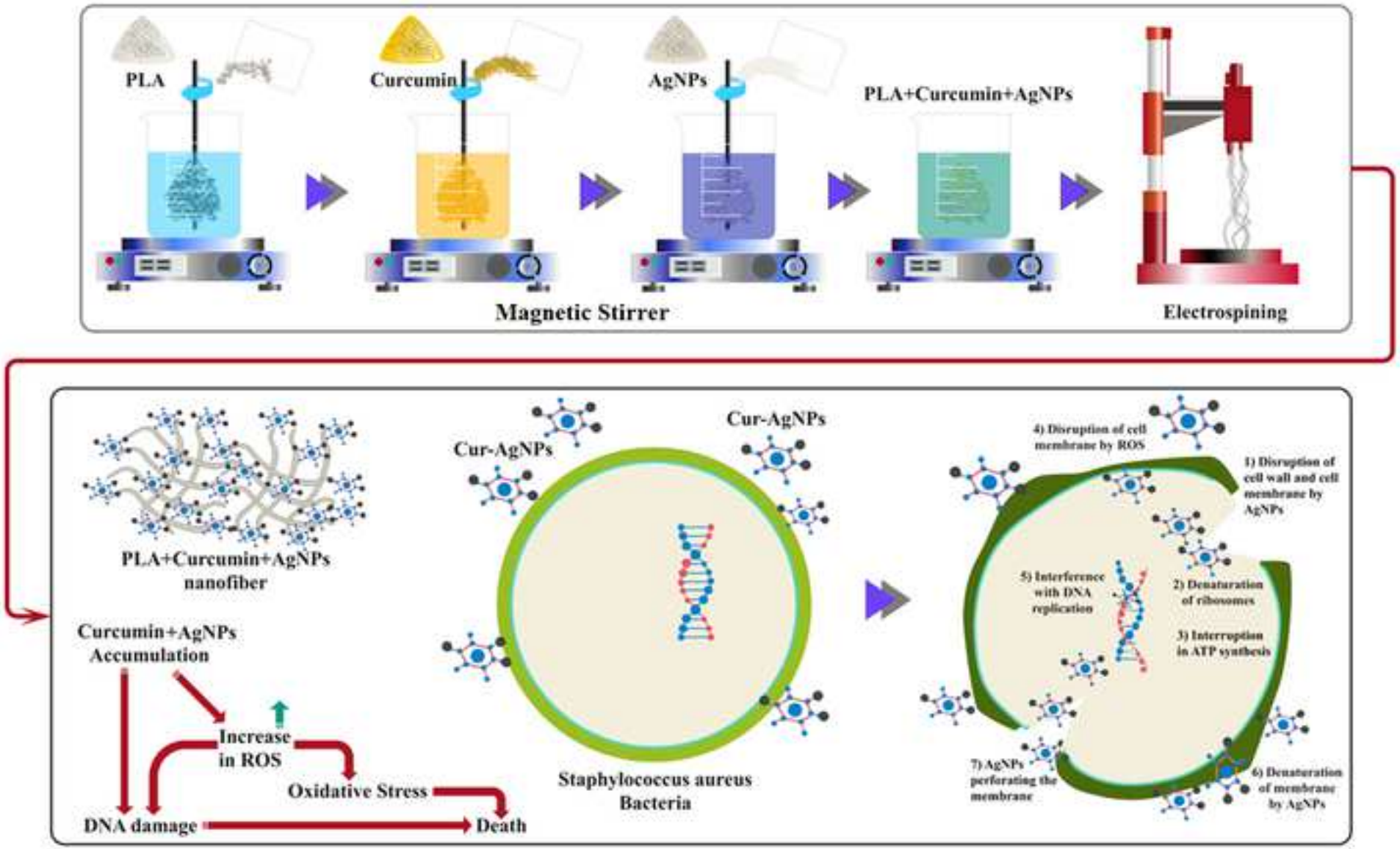

Fig. 1

Click here to access/download;Figure (300 dpi and editable format);Fig. 1..tif

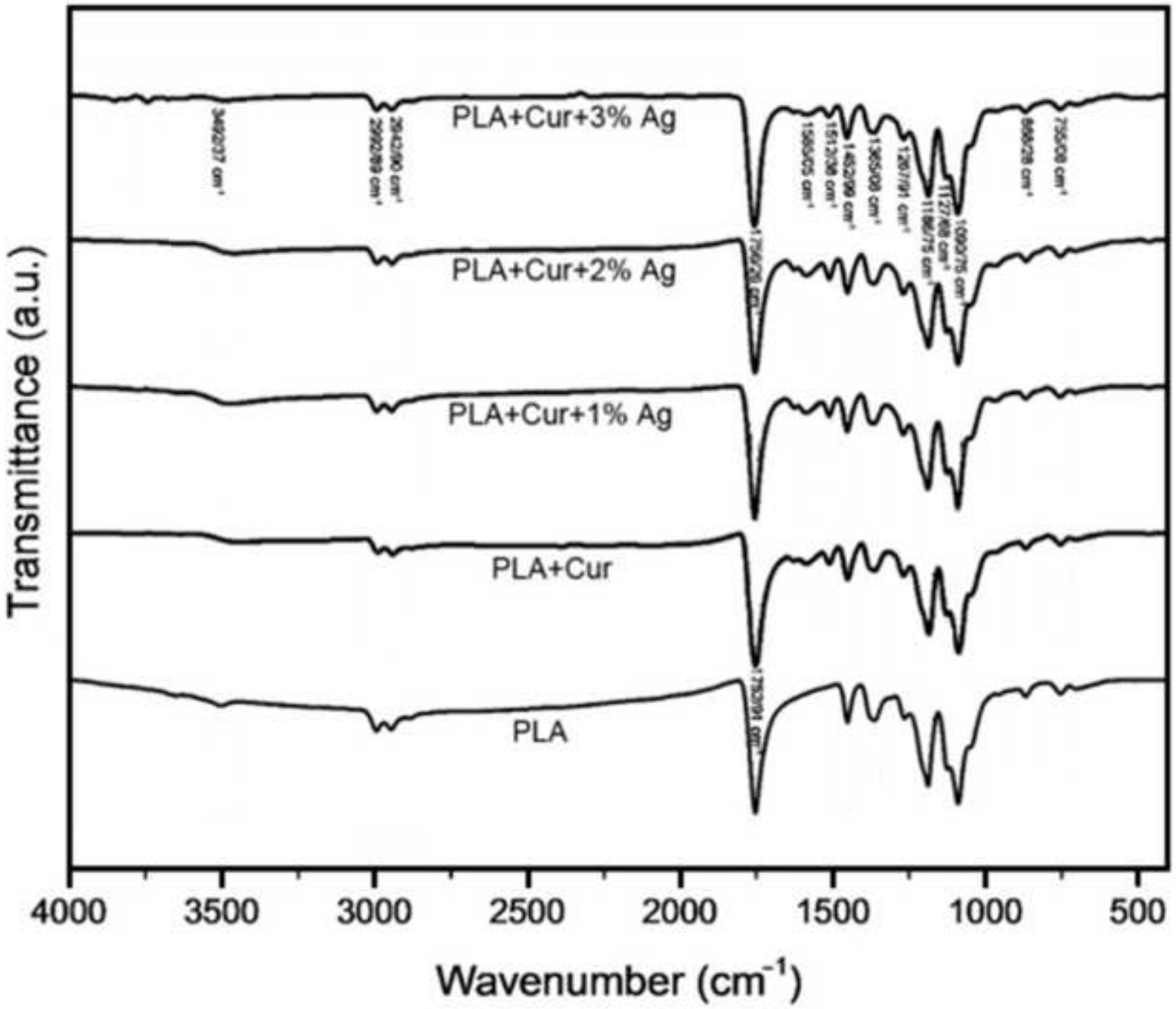

Fig. 2

Click here to access/download;Figure (300 dpi and editable format);Fig. 2..tif

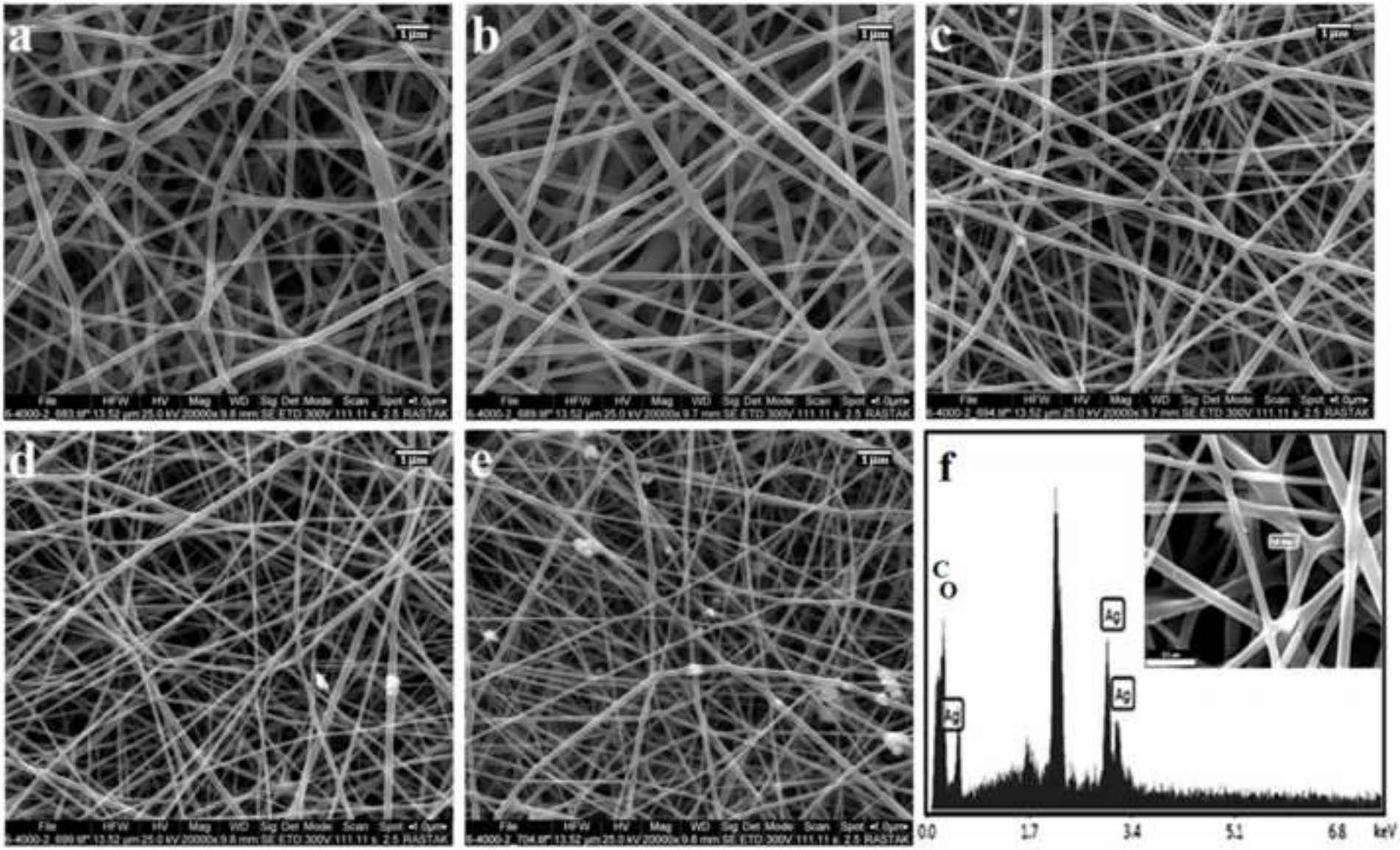

Fig. 3

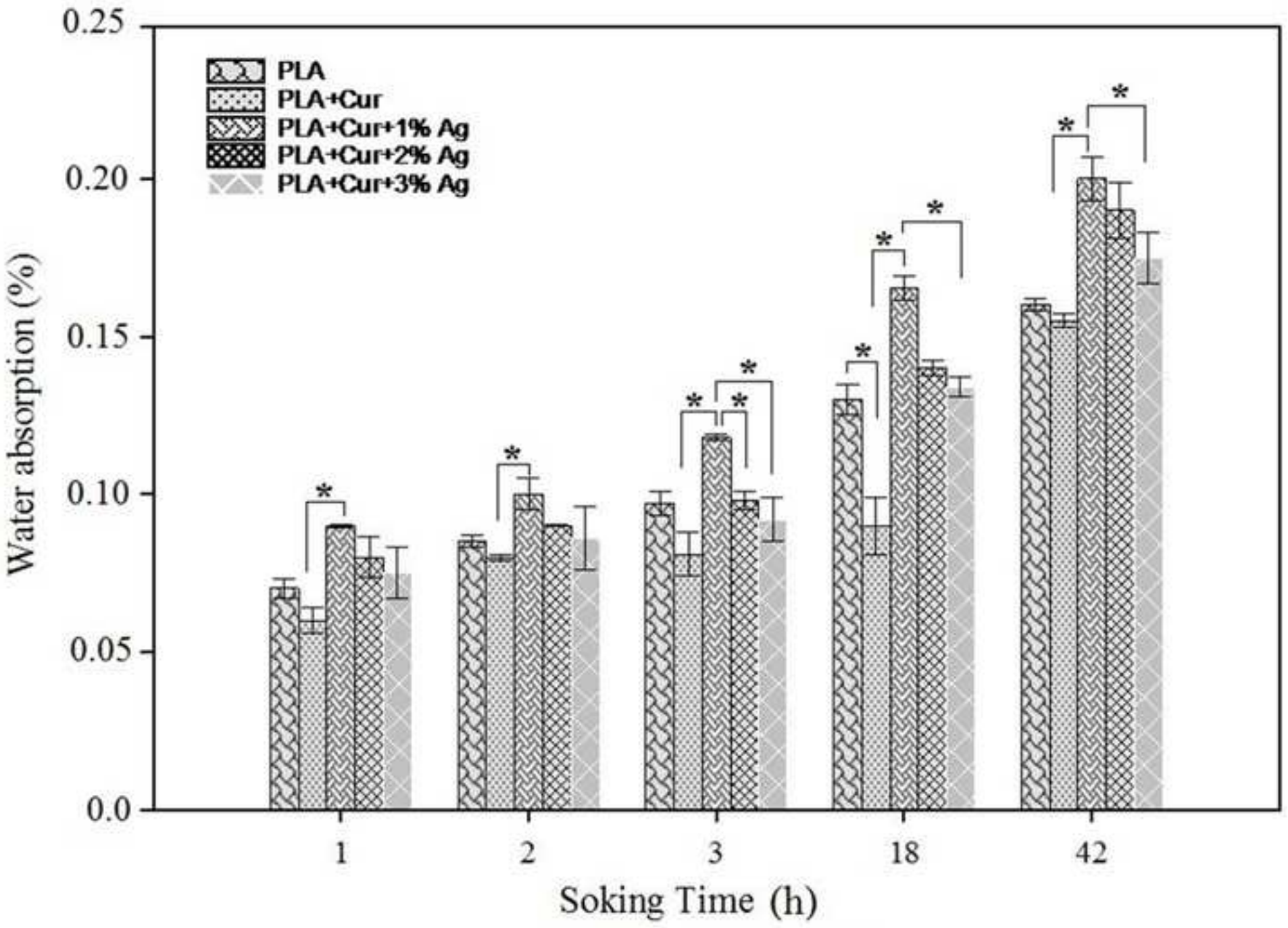

Fig. 4

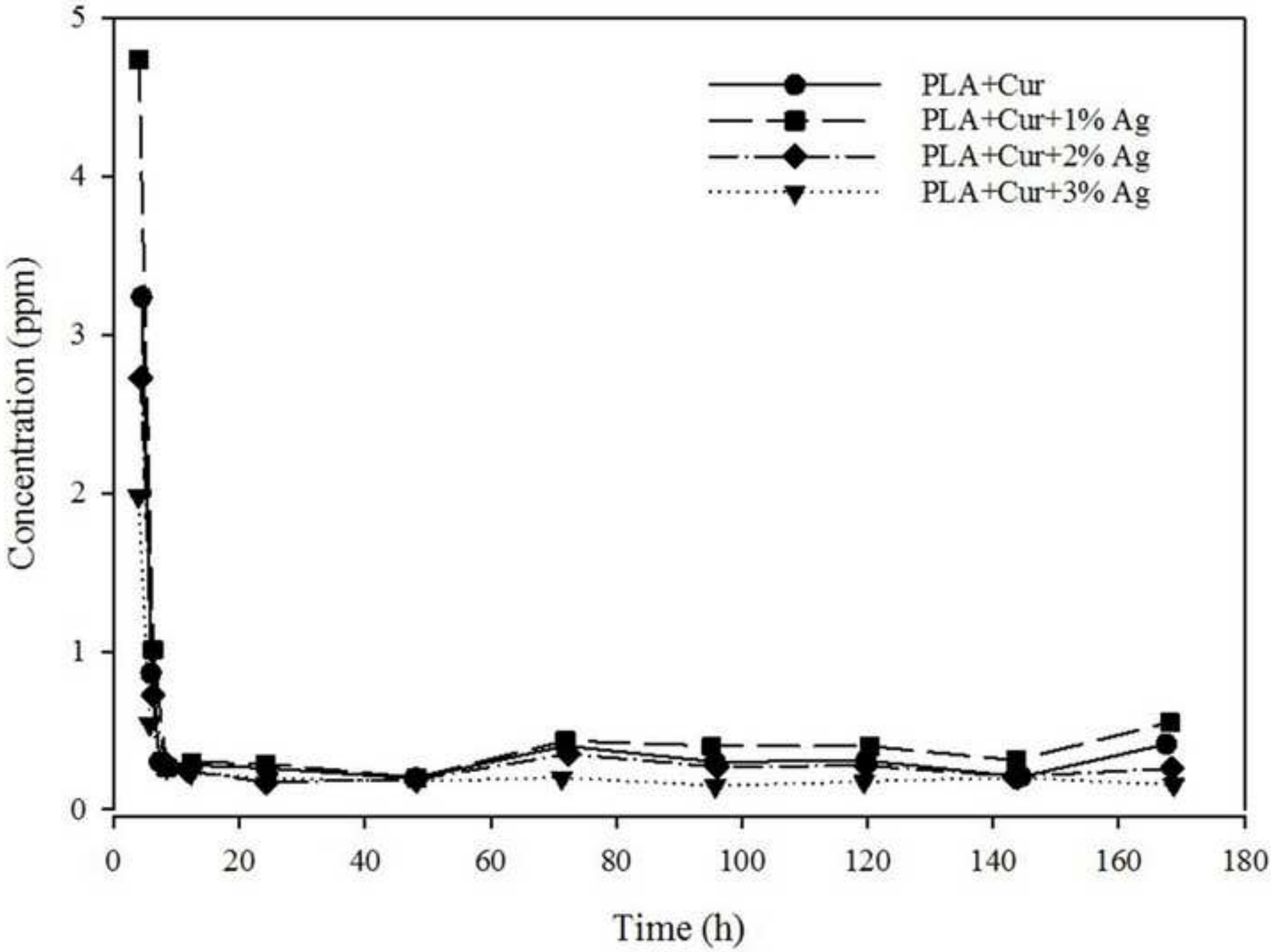

Fig. 5

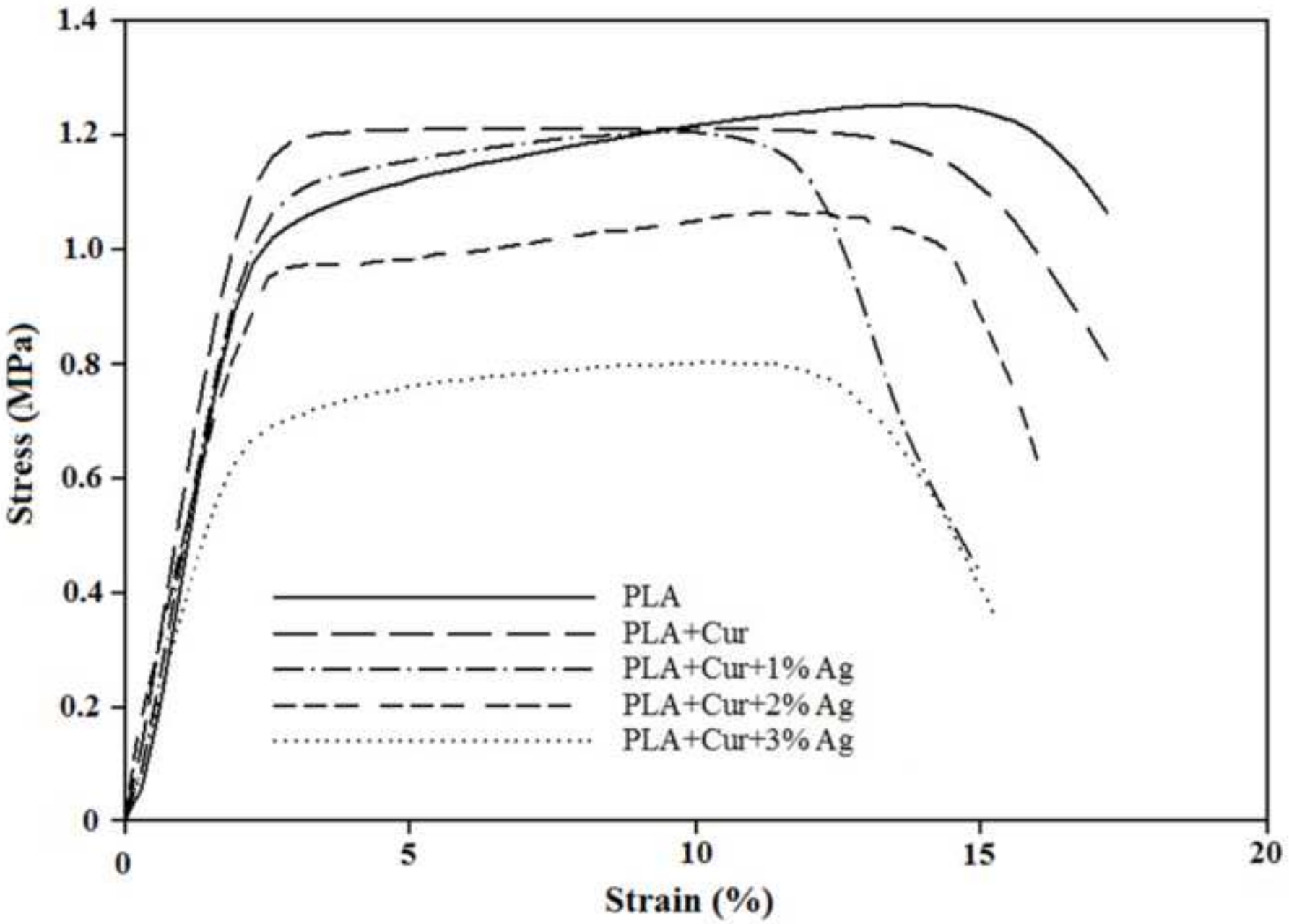

Fig. 6

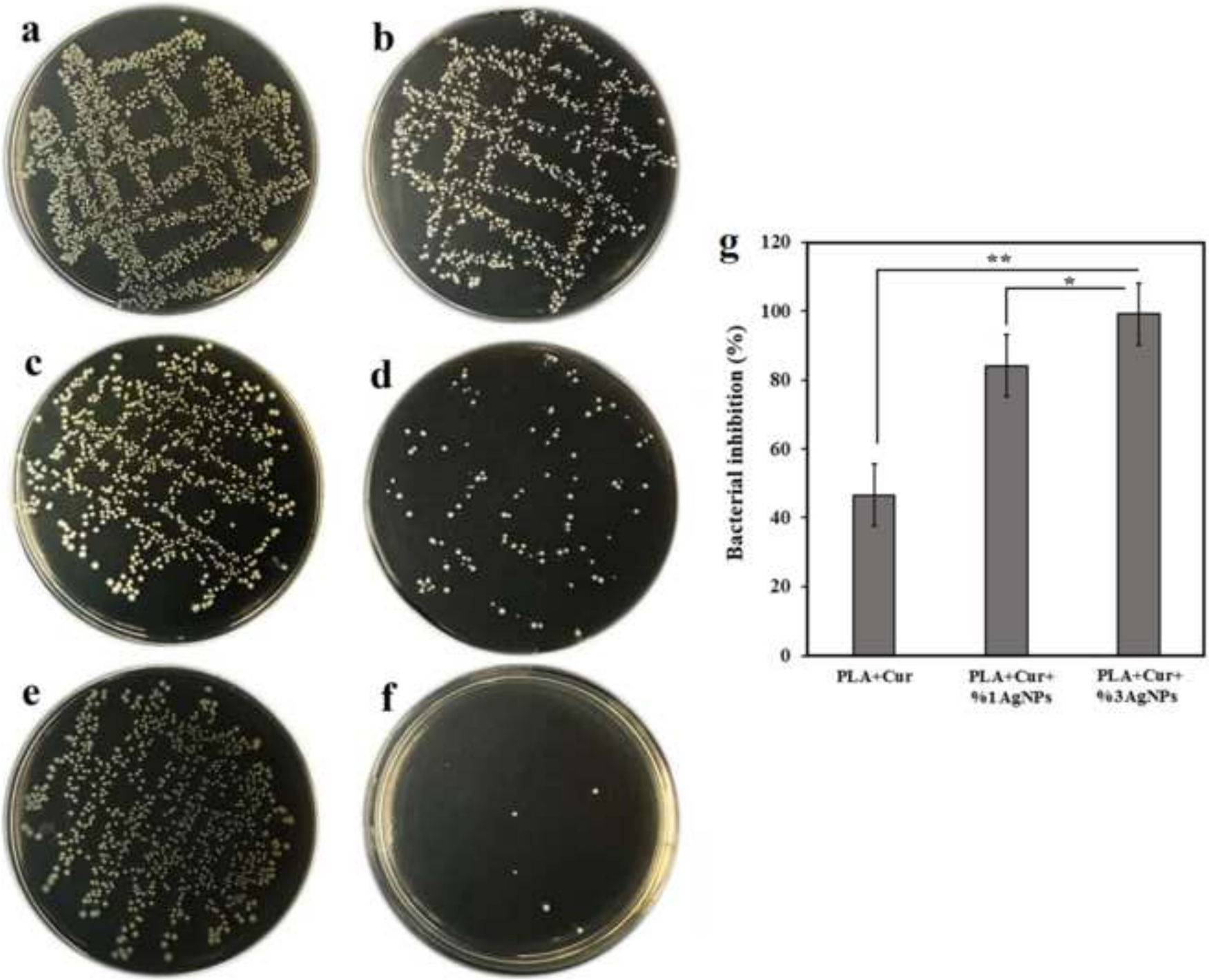

Fig. 7

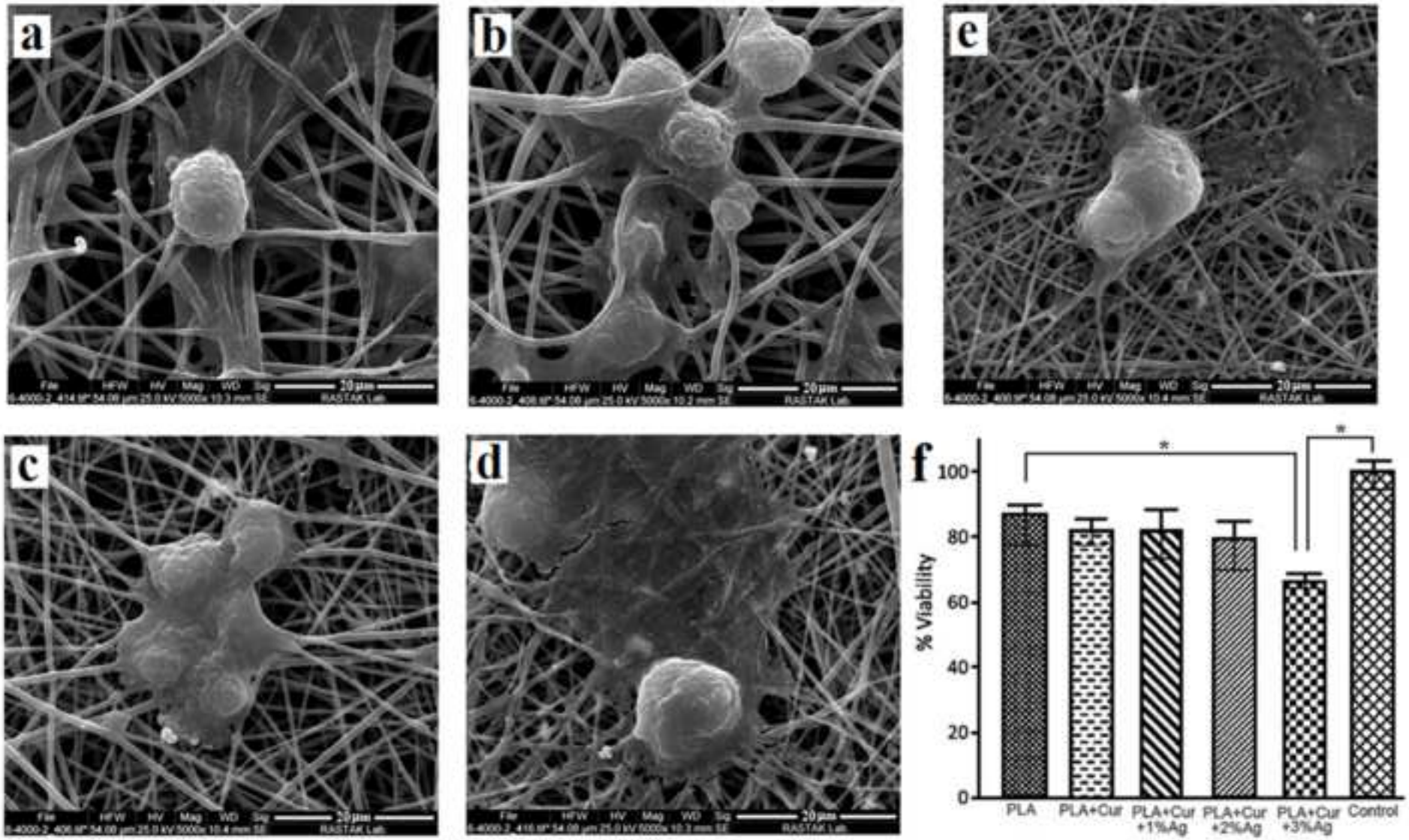

Declaration of interests

☒ The authors declare that they have no known competing financial interests or personal relationships that could have appeared to influence the work reported in this paper.

Author Statement

All persons who meet authorship criteria are listed as authors, and all authors certify that they have participated sufficiently in the work to take public responsibility for the content, including participation in the concept, design, analysis, writing, or revision of the manuscript. Furthermore, each author certifies that this material or similar material has not been and will not be submitted to or published in any other publication before its appearance in the Burns.

Author Contributions: Methodology, formal analysis, writing—original draft preparation, **M. Moayedi, M.T. Dehaghani, S. Shojaei, S. Z. Benisi**; Conceptualization, supervision, writing—review and editing, **T. Ahmadi, V. Nekouie, H.R. Bakhsheshi-Rad**. All authors have read and agreed to the published version of the manuscript.

Preparation and assessment of polylactic acid-curcumin nanofibrous wound dressing containing silver nanoparticles for burn wound treatment

Mehri Moayedi [a], Tahmineh Ahmadi[a,*], Vahid Nekouie[b,c] , Majid Taghian Dehaghani[d], Shahrokh Shojaei[a], Soheila Zamalui Benisi[a,e] , Hamid Reza Bakhsheshi-Rad[f,*]

[a]Department of Biomedical Engineering, Islamic Azad University, Central Tehran Branch, P.O. Box 13185/768, Tehran, Iran
[b]Department of Engineering and Mathematics, Sheffield Hallam University, Sheffield, S1 1WB, UK
[c]Materials and Engineering Research Institute (MERI), Sheffield Hallam University, Sheffield, S1 1WB, UK
[d]Department of Materials and Metallurgical Engineering, Abadeh Higher Education Centre, Shiraz University, Abadeh, Iran
[e] Stem Cells Research Center, Tissue Engineering and regenerative Medicine Institute, Ventral Tehran Branch, Islamic Azad University, Tehran, Iran
[f]Advanced Materials Research Center, Department of Materials Engineering, Najafabad Branch, Islamic Azad University, Najafabad, Iran

*****Correspondence: tahmadi56@yahoo.com (T.A); rezabakhsheshi@gmail.com (H.R.B.-R.)

Abstract

This study aims to produce and evaluate nanofibrous wound dressings through the electrospinning method, utilizing polylactic acid (PLA), curcumin (Cur), and silver nanoparticles (AgNPs). For this purpose, five types of wound dressings with PLA, PLA+Cur, PLA+Cur+1%AgNPs, PLA+Cur+2%AgNPs and PLA+Cur+3%AgNPs were produced using the electrospinning method. Analysis of the Fourier transform infrared spectroscopy and scanning electron microscopic observations indicated the successful fabrication, with nanometer diameters achieved in all electrospun samples. The examination of water absorption of wound dressings revealed that during 40 h, the electrospun samples had variable water absorption between 0 and 0.25%. The results of the curcumin release test over one week showed that the nanofibers with PLA+Cur+2%AgNPs exhibited the lowest release rate, while those with PLA+Cur+3%AgNPs showed the highest release. The assessment of mechanical properties revealed that the tensile strength of nanofibers increased by adding curcumin to polylactic acid, while the addition of a high content of AgNPs led to a decrease in tensile strength. Also, the PLA+Cur wound dressing demonstrated 84.06% and the one with PLA+Cur+3%AgNPs exhibited 99.12% antibacterial properties. The cell culture test demonstrated that the incorporation of curcumin and AgNPs, both the growth and proliferation, as well as the adhesion on the nanofibrous wound dressing, increased well. Thus, the

PLA+Cur+1%AgNPs nanofibrous scaffold, as a multipurpose dressing, presented considerable promise for wound healing and burn treatment.

Keywords: Nanofibrous, Polylactic acid, Curcumin, Silver nanoparticles, Wound dressing, Electrospinning.

1. Introduction

The problems of bacterial infections causing chronic wounds threaten the lives of numerous patients and therefore require specialized treatment and care methods. Meanwhile, the improper use of antibiotics has resulted in a significant increase in bacterial resistance [1, 2]. One approach to overcome this problem involves the localized release of the drug and the utilization of wound dressings with antibacterial properties. Although the use of synthetic polymer scaffolds is prevalent in the medical field due to their biocompatibility and biodegradability, these materials usually do not have inherent antimicrobial properties. Nevertheless, they can be used as carriers for drugs or be combined with other antimicrobial substances [3-5]. Fibrous scaffolds based on polylactic acid offer valuable advantages for wound healing and tissue regeneration. Their unique features, such as high porosity, high surface area to volume, surface morphology, and fibrous diameter, which can be controlled by adjusting the parameters of the electrospinning process, make them suitable for these applications [2, 6]. On the other hand, in the electrospinning process, incorporating various suitable materials and making a nanocomposite scaffold can overcome the limitations of synthetic polymers. This enables the scaffold to acquire unique properties, such as antibacterial features and drug delivery capabilities [7-9]. It is important to keep in mind that different variables during electrospinning processing affect the shape of fibrous, comprising their diameter, porosity, and surface structure. These variables involve the operating distance in the electrospinning device, spinning voltage, solution feeding rate, needle inner size, and suspension viscosity, which is governed by the polymer content and additives [9-11]. It has been found that as the solution jet travels from the needle to the metal collector, it may split into multiple jets, resulting in a uniformity of fibrous diameters [9-11]. Regarding the additive for PLA-based nanofibrous scaffolds, curcumin has been extensively employed to cure several illnesses and skin conditions [10]. Curcumin possesses noteworthy properties in wound healing due to its anti-inflammatory, antioxidant, anti-cancer, anti-coagulant, and anti-infective effects, which accelerate the natural wound healing process at different stages. Recent studies indicate that curcumin can

reduce the body's natural response to skin wounds, including inflammation and oxidation [11]. Studies have been conducted on the use of curcumin in combination with other polymers. The results demonstrate the outstanding biocompatibility of curcumin loaded in nanofibers for wound applications. Curcumin has the potential to induce cell proliferation and enhance the process of wound healing [11, 12]. Curcumin is useful in eliminating reactive oxygen species, which promotes the accumulation of collagen in the development of granulation tissue and quickens the closure of wounds, both of which hasten the course of healing [12, 13]. Since curcumin exhibits low solubility in water compared to polymer, processing it in order to render it accessible for applications necessitates the use of micro and/or nanomaterials [14, 15]. Also, according to the research, PLA nanofibers loaded with curcumin exhibit favorable therapeutic properties. PLA and poly lactic-co-glycolic acid (PLGA) nanofibers containing curcumin are suitable materials for drug delivery, demonstrating effectiveness against cancer in laboratory conditions [16]. Accordingly, adding AgNPs to curcumin may substantially boost its antibacterial performance towards both Gram-positive and Gram-negative bacteria [17, 18]. In another study, the antimicrobial properties of AgNPs were reported in relation to the growth of *E. coli* cultured on agar plates. The results obtained show that the inhibition is dependent on both the concentration of AgNPs and the initial number of cells used in the experiments [19]. Silver has a strong antibacterial effect by causing damage to the DNA in the microorganism cell [20]. In addition to antibacterial activity, research has concentrated on exploring the therapeutic properties of silver and its nanoparticles, which has resulted in the development of various wound dressings with enhanced antibacterial effects. It has been demonstrated that activated carbon fibers containing silver increases the proliferation of fibroblasts in the skin. It has also been proven that prolonged exposure of epithelial cells to silver nanoparticles stimulates them to secrete TGF-β [17, 18, 20]. AgNPs solution was used for treating superficial wounds, revealing that this treatment accelerates wound healing in a shorter time and with better skin regeneration [21, 22]. Another study aimed to investigate the wound-healing potential of collagen nanofibrous dressings containing silver nanoparticles. The in vivo study revealed an accelerated speed of wound healing of composite nanofibrous wound dressings compared to non-composite collagen nanofibrous. Ulcerological analysis showed an acceleration in re-epithelialization, collagen production, and improved wound contraction with AgNPs composite collagen nanofibrous [22-24].

Considering the limitations of synthetic polymers and, on the other hand, as mentioned, acknowledging the special characteristics of curcumin and silver nanoparticles, the current research focused on developing a multi-component nanofibrous wound dressing with the electrospinning technique. The dressing was created from a combined solution of polylactic acid, curcumin, and silver nanoparticles with different concentrations, intended for burn treatment and wound dressing applications. The fabricated nanofibrous wound dressings were assessed through various methods, including Fourier transform infrared spectroscopy (FTIR), scanning electron microscopy, water absorption testing, drug release rate measurement, bacterial assays, mechanical properties testing, and cell culture analysis to observe morphological, moisture, and antibacterial behavior.

2. Materials and methods

2.1. Materials and electrospinning process

The electrospinning solution was prepared by polylactic acid $(C_3H_4O_2)_n$ granules with a nominal size of 3 mm and a molecular weight of 60000 g/mol from SIGMA, curcumin ($C_{21}H_{20}O_6$, MW = 368.38, Xiya Reagent Co., Ltd., China) with a molecular weight of 368.38 g/mol from Merck, and silver nanoparticles (AgNPs, 99.99% purity) with a particle size of 20 nm from US Research Nanomaterials, Inc. In addition, dichloromethane (DCM, Merck) and dimethylformamide (DMF, Merck) were employed as solvents.

In order to prepare a solution of 15 wt% PLA (Sample No. 1), 1.5 gr of PLA, previously dried in an oven at 70°C for 2 h, were thoroughly mixed using an electric stirrer with 7 mL of dichloromethane and 3 mL of dimethylformamide for 40 min. In the next step, sample solution 2, PLA+Cur was prepared by initially preparing two distinct solutions. The first solution involved dissolving 1.5 gr of dried polylactic acid in 7 mL of dichloromethane and the second solution contained 2.2 gr of curcumin dissolved in 3 mL of dimethylformamide solvent. Following preparation, these two solutions were combined and placed on the stirrer again for further mixing. Ultimately, to produce fibrous PLA+Cur+1 wt.% AgNPs (containing 0.015 gr Ag; sample 3), PLA+Cur+2 wt.% AgNPs (containing 0.03 gr Ag; sample 4), and PLA+Cur+3 wt.% AgNPs (containing 0.045 gr Ag; sample 5), 1wt.% Ag (0.015 gr Ag), 2 wt.% Ag (0.03 gr Ag), and 3 wt.% Ag (0.045 gr Ag) were added to the previously prepared PLA+Cur solution. To ensure complete suspension of the nanoparticles, each solution was placed on a stirrer for 2 h (Scheme. 1).

For the electrospinning process, the prepared solutions were transferred into 5 ml syringes with a G22 needle. Subsequently, the tip of the syringe needle and an aluminum foil as a collector were positioned at a distance of 15 cm from each other. The voltage difference between the tip of the needle and the aluminum foil was adjusted to 20 kV, and the flow rate was set to 0.5 mL/h. Electrospinning was carried out for 4 hours to achieve optimal results, ensuring the production of uniform fibers without bead formation by observing through a light microscope. During electrospinning, the solvents evaporated, leaving only the fibers adhered to the aluminum foil.

Scheme. 1.

2.2. Characterization

To identify functional groups and bonds formed in the electrospun samples, infrared spectroscopic analysis (PerkinElmer, USA) was employed within the wavelength range of 400-4000 cm^{-1}. The surface morphology of the electrospun samples was examined utilizing a scanning electron microscope (ESEM, Quanta 200, FEI). The mean and distribution of fibrous diameter was determined by measuring fibrous diameter in SEM micrographs with image processing software (Image J, National Institutes of Health, USA). Also, to ascertain the type and percentage of elements, Energy Dispersive X-ray Spectroscopy (EDAX analysis) was utilized. The mechanical behavior of the electrospun samples was measured using a universal tensile testing machine (SANTAM-20, Iran). Each tensile test was performed at room temperature using a crosshead speed of 5 mm/min. The findings were presented in the form of stress-strain curves.

The water absorption capability of the electrospun samples was tested at intervals of 1, 2, 3, 17, and 40 h. For this purpose, pieces of the sample with dimensions of 1×1 cm^2 were prepared and weighed using a scale with an accuracy of 0.0001 gr. The prepared samples were inserted in falcon tubes containing 5 cc of distilled water. Then, the falcon tubes were placed in an incubator with a temperature of 37 ^{o}C. After the specified period, the samples were taken out from the incubator, their surface water was filtered through filter paper, and their weight was re-measured using a scale. At the end, the amount of water absorption or swelling rate (S_w) of the samples was calculated according to Eq. 1.

$$S_w = (W_1 - W_0)/W_0 \quad (1)$$

where W_0 is the dry weight of the sample and W_1 is the weight of the wet sample after absorbing water.

2.3. Drug release test

For the release test, electrospun samples containing curcumin in dimensions of 1×1 cm^2 were used. The electrospun samples were placed in Falcon tubes containing 5 cc of distilled water and phosphate-buffered saline, supplemented by Tween 80 (Polysorbate 80, polyoxyethylene sorbitan monooleate), at concentrations of 5 to 100 ppm (via dilution). Then, the Falcon tubes were placed in the refrigerator for durations of 4 to 168 h. After each time interval, the samples were taken out of the solution and transferred into the same amount of solution in a new falcon tube, ready for the subsequent time interval. The preceding solutions were stored in the refrigerator. It should be noted that initially, the maximum absorption wavelength for curcumin was determined to establish a calibration line. Finally, their absorption at the maximum absorption wavelength (423 nm) was determined using the equation derived from the curcumin drug calibration line. The amount of light absorption of different samples was measured using ultraviolet spectrophotometry (UV-Vis, LAMBDA 750, PerkinElmer). Curcumin release was evaluated for each sample, and a cumulative graph was plotted against time. Thus, the concentration graph was generated according to the absorption rate of curcumin in distilled water and phosphate-buffered saline.

2.4. Antibacterial test

In this study, *Staphylococcus aureus* was employed to evaluate antibacterial activity. The antibacterial activity of the sample was assessed using the colony-forming unit (CFU) method. The samples were sterilized with 70% ethanol and a physiological solution. Subsequently, a bacterial suspension was prepared according to the McFarland standard, and its optical density (OD) was measured at a wavelength of 630 nm. Then, 1000 microliters of the bacterial suspension were poured on the blank samples, followed by an incubation period of 24 h at 37±1 °C. After the mentioned period, dilution was carried out at a ratio of 1:10, and the diluted bacteria were plated onto a nutrient agar culture medium. The plates were then incubated for 18 h at 37 ± 1 °C. The average number of colonies after incubation was determined using the ImageJ program, and the antibacterial efficacy of the sample was reported as a percentage according to Eq. 2.

$$R(\%)=(N_A-N_B)/N_A \times 100 \quad (2)$$

where R (%) represents the antibacterial effectiveness of the sample in percentage, N_A is the number of colonies in the sample before exposure to the antibacterial agent, and N_B is the number of colonies in the sample after exposure to the antibacterial agent.

2.5. Cytotoxicity assay

In this assay, L929 cells (NCBI C161) sourced from the cell bank of the Pasteur Institute of Iran were utilized. Culturing the cell was performed in a humidified environment with 5% CO_2 at 37 °C, and the culture media were replenished every 48 h. When the cells reached 80 to 90% confluency, they were detached using 0.25% trypsin/EDTA and then sub-cultured at a density of 10^5 cells per cm^2 in a 100 mm petri dish. Cells from the 3rd-6th passage of L929 cells were utilized for the tests. All cell assay experiments were performed in triplicate for every sample type at every time point, and the experiments were repeated at least once. The cell viability assay was conducted employing an indirect contact technique. The L929 cells were seeded in a 96-well plate at a density of 2×10^4 cells per mL with 100 µL of suspension for every well and incubated for 24 h to allow attachment. Following this step, the culture medium was removed and 100 microliters of MTT (dimethyl thiazyl diphenyl tetrazolium bromide test, MTT, Sigma, USA) solution, with a concentration of 0.5 mg/ml, was added to each well and placed in an incubator for 4 h. After the 4-h incubation period, the solution was removed from the cells, and isopropanol was added to dissolve the purple formazan crystals. To facilitate better dissolution of the MTT sediment, the plate was placed on a shaker for 15 min. Then, the concentration of the substance dissolved in isopropanol was determined using an ElizaReader device (BioTek ELx808, USA) at a wavelength of 570 nm. The well with more cells exhibits a higher optical density (OD) compared to the well with fewer cells, according to Ref. [25].

2.6. Statistical analysis

The mean value ± standard deviation was used to display the data analysis. Software designated GraphPad Prism (V.8) was used to perform statistical analysis. When $*p < 0.05$ and $**p < 0.01$, the data differences were considered statistically significant.

3. Results and discussion

3.1. FTIR spectra

The FTIR spectra for PLA, PLA+Cur, PLA+Cur+xAgNPs nanofibrous samples are shown in Figure 1. In the spectrum of the polylactic acid-curcumin-AgNPs sample, the broad peak at wavenumber 3463 cm^{-1} is attributed to either the stretching vibration of O–H in the curcumin structure or to the adsorbed water [26]. The peaks at wavenumbers of 2929 cm^{-1} and 2942 cm^{-1}, respectively, are related to the asymmetric and symmetrical stretching vibrations of C–H in the

aliphatic structures of PLA and curcumin [27]. Also, the peaks observed at wavenumbers of 1756 cm^{-1} and 1585 cm^{-1}, respectively, correspond to the stretching vibrations of C=O bonds in the carbonyl and carboxyl structures in PLA and curcumin, and the stretching vibration of C=C in the aromatic rings of curcumin [28]. In addition, the peaks at wavenumbers of 1452 cm^{-1}, 1365 cm^{-1}, and 1186 cm^{-1} are attributed to the bending vibrations of C–H in methyl and methylene groups, and the stretching vibration of the C–OH bond in the curcumin structure, respectively [29]. Furthermore, the peaks detected at wave numbers 1090 cm^{-1} and 888 cm^{-1}, respectively, are related to C–O–C stretching vibration in PLA and twisting vibration of C–H in curcumin and PLA structure [28-30]. Finally, after introducing AgNPs, a shift of the chitosan (CS) peaks at 3356 cm^{-1} was noticed, which is explained by the interaction of the reduced Ag with CS. Additionally, the hydroxyl peak's strength was found to have decreased. Therefore, as indicated by the FTIR test results, the presence of PLA, curcumin, and AgNPs in these composites is evident.

Fig. 1.

3.2. Microscopic evaluation

Figure 2 shows the SEM images of PLA, PLA+Cur, and PLA+Cur+xAgNPs nanofibrous samples. As can be seen from Figure 2a, the PLA electrospun nanofibrous scaffold has no beads, appropriate morphology, and a uniform diameter distribution, with an average diameter of 218 nm, along with uniform void space. However, the aforementioned parameters are constants in the present study. As seen in Figure 2b, the PLA+Cur electrospun nanofibrous scaffold has no beads, uniform void space, and an average fibrous diameter of 240 nm. It is worth mentioning that the addition of curcumin results in a color change in the fibrous, which is observable to the naked eye; the lighter, somewhat yellow coloration observed on the electrospun wound dressing indicates the presence of curcumin, which is effectively dispersed among the fibrous [31-33]. As evident from the comparison to PLA nanofibers, the presence of curcumin results in fibers that are more uniform and continuous, with void spaces that also have a better fit. Additionally, there is no visible accumulation of curcumin on the surfaces. Hence, it is evident that increasing the amount of curcumin in PLA substantially reduces the diameter of the nanofibers and improves the uniformity of the fibers. An interconnected porous structure, formed by loosely stacked nanofibers, was observed. In Figures 2c-e, respectively, SEM images of PLA, PLA+Cur, and PLA+Cur+xAgNPs nanofibrous samples can be seen. In these images, the presence of AgNPs is clearly discernible,

and the fibers exhibit uniform distribution, appropriate diameter, and spacing. The average fibrous diameters for electrospun samples 3, 4, and 5 are 140, 135, and 117 nm, respectively, indicating a decrease in fibrous diameter due to the presence of AgNPs. The smooth fibrous with regular morphology and relatively narrow dimensional distribution, which were smaller than pure PLA fibrous, can be due to the increase in conductivity of the solution resulting from the addition of AgNPs [33]. AgNPs with high electrical conductivity are being incorporated, and this dramatically raises the conductivity of the polymer solution, which escalates electric charges and reduces the diameter of the polymer fibers. In this context, elevating the solution's conductivity could yield a significantly more homogenous fibers combined with a decrease in the fibrous diameter [18]. To confirm the presence of AgNPs, EDX analysis was conducted on PLA+Cur+3%AgNPs nanofibrous sample. The result of this test is presented in Figure 2f. As evident from this spectrum, the strong peak confirms the presence of silver in this electrospun sample.

Fig. 2.

3.3. Water absorption evaluation

Figure 3 displays the bar graph illustrating the water absorption of PLA, PLA+Cur, and PLA+Cur+xAgNPs nanofibrous samples at various soaking times. As can be seen, the water absorption of all five wound dressing samples varies from 0.0004 to 0.0045 gr samples over the 40 h testing period. In the initial sample containing only PLA polymer, the water absorption varied over time, so that at certain intervals, there was either a negligible increase in weight or no change at all, indicating its hydrophobic nature. S. Krishnamohan et al. [34] displayed that the water absorption of pure PLA film varied from 0% to 0.02% during a 10-day experiment. Furthermore, the composite exhibited varying degrees of water absorption, with fluctuations occurring unevenly during the experiment. The utilization of PLA as a hydrophobic component was confirmed by test results, indicating its substantial resistance to water. Surface modification of PLA with plasma can enhance the hydrophilicity of the polymer. In the PLA+Cur sample, a wound dressing containing curcumin, the fluctuation in water absorption was more pronounced, likely attributable to the hydrophobic nature of curcumin, with a significant reduction in water absorption with time extension. In the PLA+Cur+1%AgNPs sample, which is a combination of fibers with curcumin and AgNPs, there was a very small increase in water absorption, rising from 0.0011 to 0.0036 gr. Research has shown that integrating curcumin into a nanoparticle-polymer composite could offer an alternative and easier approach to enhancing the solubility of curcumin in the water while

diminishing its hydrophobic characteristics [35]. In the PLA+Cur+2%AgNPs sample, the augmentation of AgNPs intensified hydrophobicity, consequently resulting in a decrease in water absorption once more. Regarding the PLA+Cur+3%AgNPs nanofibrous, with a further addition of AgNPs, water absorption has decreased. As evident from the graph, the addition of curcumin led to a reduction in water absorption, attributed to its inherent hydrophobic nature. Subsequently, with the incorporation of AgNPs, further fluctuations in water absorption occurred, arising from the presence of AgNPs within the polymer matrix and their hydrophobic properties. In this context, significant differences between the water absorption percentages of PLA+Cur+1%AgNPs and PLA+Cur nanofibers were observed ($p < 0.05$). In general, it is observed that as the quantity of AgNPs increases, water absorption decreases further.

Fig. 3.

3.4. Drug release behavior

Figure 4 displays the curves illustrating the changes in released curcumin for various samples during the immersion time. According to this diagram, the release of curcumin was notably high within the first 4 h in all the samples. However, with the passage of time, there was a tendency for the released curcumin to diminish. As indicated by this diagram, the strongest release of curcumin within the first 4 h was related to PLA+Cur+1%AgNPs, followed by samples PLA+Cur, and nanofibrous containing 2 and 3% AgNPs. Furthermore, according to this figure, for PLA+Cur+3%AgNPs sample, between approximately 145 and 168 h, there was an increase in the release of curcumin again. Indeed, in the PLA+Cur+3%AgNPs sample, the lack of strong release during the initial immersion periods suggests that the drug was stored within the carrier. Accordingly, this stored drug was subsequently released for longer periods of time. The structure of nanofibers facilitates a sustained and controlled release of curcumin over time. Due to the low degradation rate of PLA, the release mechanism often involves the diffusion of curcumin through the PLA matrix. However, there was no significant difference between curcumin release for PLA+Cur and PLA+Cur+3%AgNPs nanofibrous samples between 15 and 168 h ($p > 0.05$). Hemostasis, inflammation, growth, and reconstruction are the four interaction phases of the wound repair procedure, during which time fresh skin tissue may develop. Even while wounds recover in an orderly fashion, chronic wounds might result in an unfinished, drawn-out process of recovery that does not restore integrity. Under these circumstances, there is an overabundance of oxidative

stress, which fuels more oxidative stress and prolongs inflammation. Consequently, curcumin's short-term release may aid in the repair of wounds due to its anti-inflammatory and antioxidant characteristics. A continuous release of curcumin (81.5%) from CS-polyethylene glycol NPs was reported. The histologic examination demonstrated increased collagen and granulation tissue production, which hastens the repair of wounds [25].

On the other hand, the stability of nanoparticles is an important parameter for both biological applications and storage. The evolution of curcumin in chitosan /polyvinyl alcohol/sodium alginate (CS/PVA/SA) hydrogels with various combinations of Ag_2O/SiO_2 nanoparticles was investigated. It was demonstrated that in hydrogels without NPs, the evolution of curcumin occurred rapidly, reaching its peak within 16 h, and after that, no significant further evolution of curcumin was observed. By adding and increasing the percentage of nanoparticles in the hydrogel, the release of curcumin became slow, continuous, and balanced [36]. The porosity of the NPs and the bonds that occurred between curcumin and the nanoparticles as the hydrogel's NPs amount grew were responsible for the slow, steady, and balanced synthesis of curcumin. Conversely, when the proportion of NPs rose, these bonds became more prevalent, which decreased the amount of drug release. Additionally, a number of curcumin molecules became trapped in the porosity of hydrogels and NPs, which resulted in their partial release from the hydrogel structure.

Fig. 4.

3.5. Mechanical behavior

The stress-strain curves for different samples are presented in Figure 5. As evident, the addition of curcumin to PLA has resulted in an increase in nanofibrous tensile strength, which subsequently decreases with higher percentages of AgNPs. The increase in tensile strength upon adding curcumin to polylactic acid indicates good miscibility between these two substances, which implies that there is a significant interaction between curcumin and PLA. In a study, it was observed that in the first step, the addition of curcumin resulted in the formation of a random "beads fibrous" feature in the fibrous; however, no chemical reaction occurs between curcumin and PLA based on the FTIR results. Several studies have considered such an irregular formation. Such an irregular formation characterized by the "beads fibrous" feature may be due to the low solubility of curcumin, leading to accumulation during preparation, and generally, the tensile modulus and fibrous strength increase with increased molecular orientation, average molecular weight, and crystallization. The strength and modulus of PLA decrease with an increase in the

amount of curcumin in the matrix, so that when curcumin is added at 5% of the weight, the strength and modulus decrease by 35% and 37%, respectively [37]. On the other hand, nanoparticles act as stabilizers by linking polymer chains and preventing them from breaking. In a study, to be able to look into the impact of the weight fraction of nanoparticles, the distribution of atomic strains was compared between pristine nanofibers and those loaded with AgNPs in two concentrations (3.9% and 5.8%). Although the elastic performance of nanofibers loaded with 3.9% AgNPs is relatively greater compared to the sample containing 5.8% AgNPs, potentially owing to local strain near the added NPs, the enhancement in fracture resistance is significantly greater with the 5.8% sample. It's worth noting that the outcomes likewise depend on the placement at which the nanoparticles are released. Here, the nanoparticles are located in the middle of the doped nanofibers, which does not play a favorable role as the polymer chains begin to crack on one side. Nanoparticles restrict the motion of polymer chains and lessen the local atomic strain inside the nanofibrous [38]. The interactions between silver nanoparticles and the polymer matrix (PLA) can influence the molecular arrangement and chain entanglement of the polymer. Adverse interactions, such as reduced polymer chain mobility or cross-linking, may lead to a decrease in the overall mechanical strength of the nanofibrous. Interactions between curcumin and silver nanoparticles may influence their dispersion and behavior within the nanofibrous.

In another study, a set of keratin/poly(vinyl alcohol)/poly(ethylene oxide) nanofibers with different contents of AgNPs was prepared using electrospinning. Their characteristics were examined, and their outcome revealed that at a concentration of 1.2% silver nanoparticles, both the tensile strength and elongation at break reached their maximum values. The tensile properties of the composite nanofibers made with varying AgNP levels exhibited that as AgNP content rose, the tensile strength first elevated and then declined. The frequent breakdown and compaction of the nanofibers caused by the aggregation of AgNPs was likely responsible for the loss in tensile characteristics detected when the content of AgNPs exceeded 1.2%. It has been shown that AgNPs reduce the mechanical characteristics of composite fibrous [39].

However, the encapsulation of a high amount of AgNPs tends to agglomerate, forming clusters. Such clusters can serve as stress concentrators, resulting in a decrease in mechanical strength. Agglomeration may also disrupt the uniform distribution of nanoparticles within the nanofibers, thereby affecting their structural integrity. However, the strength and elastic modulus of the AgNPs-encapsulated PLA+Cur nanofibers were significantly altered by AgNPs. Overall, the

addition of 1 wt% AgNPs into PLA+Cur has a less significant effect on the strength and elongation at break, while the incorporation of 3 wt% AgNPs into nanofibers leads to a diminishment of both tensile strength and tensile strain. Due to their coarser structure and broad ranges in diameter, the electrospun nanofibers encapsulated with a high content of AgNPs are held accountable for this decrease in tensile strength. Accordingly, these findings demonstrate that the mechanical characteristics of PLA-based nanofibrous materials may fulfill dressing specifications for superior mechanical support and protection, which is crucial when applied to wound dressing utilization.

Fig. 5.

3.6. Antibacterial activity

Figures 6a-f show the antibacterial activity levels of PLA+Cur, PLA+Cur+1%AgNPs, and PLA+Cur+3%AgNPs samples relative to the blank sample against *S. aureus* bacteria. As evident from the figures, the presence of bacteria, depicted as white dots, has decreased, which indicates the destruction of the bacteria. According to the results of the CFU studies, the control specimen had a mean value of 849×10^6 CFU/mL, whereas the value of surviving *S. aureus* after 24 h of incubation was less than 108×10^6 CFU/mL following contact with the PLA+Cur specimen and 736×10^6 CFU/mL following contact with the PLA specimen. Specifically, as compared to other specimens, including the control specimen (795×10^6 CFU/mL), the PLA+Cur+Ag specimen showed the lowest bacterial activity (7×10^6 CFU/mL) against *S. aureus*.

All the nanofibrous samples exhibit higher antibacterial activity in comparison with the blank sample. Figure 6g illustrates the antimicrobial percentages that were obtained from the CFU outcomes. It is obvious from the graph that PLA+Cur+1%AgNPs have fewer bacteria than PLA+Cur, which has increased their antibacterial efficacy from 44.08% to 84.07%. When AgNPs were added, the antibacterial improvement elevated even more, reaching 99.12%. This suggests that the antibacterial decrease of the PLA-based nanofibrous is significantly impacted by the co-encapsulation of curcumin and AgNPs. Furthermore, PLA+Cur with an elevated AgNP concentration can release a bigger concentration of silver ions, which is mostly responsible for the increase in antibacterial performance when the AgNP concentration is increased from 1 to 3 wt.%. In this context, significant differences between the bacterial inhibition percentages of PLA+Cur and PLA+Cur+3%AgNPs nanofibrous were observed ($p < 0.05$). The primary cause of the effective antibacterial performance of the PLA/curcumin composite films' was curcumin's antimicrobial effects. Curcumin's primary mechanism of action is the disruption of FtsZ activity,

a protein required for bacterial survival and cell division. Curcumin has the ability to attach itself to the FtsZ protein and impede the synthesis of FtsZ protofilaments, hence impeding the development of the Z-ring, the proliferation of bacteria, and the migration of cells. It is also known that curcumin increases the FtsZ protein's GTPase function [40].

Additionally, films encapsulated with curcumin were found to have a strong antibacterial action with a high inhibitory zone toward *S. aureus*. Other studies exhibited that curcumin may prevent the growth of different bacteria in a comparable manner despite differences in cell walls. This could be owing to the fact that the antibacterial performance was linked to an augmentation of cell permeability through the process of electrostatic binding with positively charged molecules in the film [41]. The antibacterial effects of curcumin and AgNPs have been confirmed in previous research. AgNPs possess a wide range of antimicrobial properties against both fungi and bacteria, including strains resistant to antibiotics. This is because Ag, an active ingredient, has an antibacterial action. First, sulfhydryl groups within the cell wall are rapidly bound by Ag ions, which leads to the malfunctioning of these components in a variety of enzymes that contribute to the creation of transmembrane energy and fluid transport. The production of adenosine triphosphate (ATP) is then inhibited. Then, by attaching to thiol groups in areas like cytochrome oxidase and NADH-succinate dehydrogenase, Ag ions obstruct the respiratory system of bacteria, halting bacterial respiration and adenosine triphosphate generation. Lastly, by disrupting hydrogen bonds between neighboring purines and pyrimidines, Ag ions can attach to nucleotide bases and intercalate with double-stranded DNA molecules, inhibiting DNA polymerases from reproducing them [42]. AgNPs' ability to penetrate bacteria and interfere with their metabolic processes amplifies their antibacterial efficacy. There are two possible ways that Ag ions could be released: (i) polymer degradation leading to the release of non-reduced Ag ions that were formerly complexed with polymers and (ii) water diffusing through the polymer matrix and releasing Ag^{+} from nanoparticles. This modest Ag ion level may effectively have bacteriostatic impacts on *S. aureus* in vitro [43].

Furthermore, the antibacterial performance of PLA+Cur+3%AgNPs nanofibrous was higher, which may have been caused by the complementary effects of curcumin and AgNPs. It is possible that the PLA+Cur+3%AgNPs nanofibrous superior inhibitory activities against *S. aureus* were caused by its distinct cell wall structure [41]. Due to their binding to the peptidoglycan layer of bacteria, curcumin and AgNPs have been linked to bacterial destruction of membranes. Curcumin

and AgNPs have an antibacterial effect mainly because they interfere with the bacteria's DNA, proteins, and replication of cells [44].

According to Alves et al., AgNPs may improve curcumin's antibacterial activity when combined to create curcumin-AgNPs nanocomposites. Consequently, the following might be used to characterize curcumin-AgNPs primary antibacterial mechanism: Curcumin serves as a capping and reducing agent for each AgNPs, and (ii) the nanocomposites of curcumin-AgNPs bond to the bacteria to generate Ag^+ ions [45, 46]. Ultimately, the generation of Ag^+ ions results in the production of reactive oxygen species, which destroy membranes, as well as bacterial lipases, which allow intracellular contents to seep out and eventually result in bacterial death.

Fig. 6.

3.7. Biocompatibility

All materials that are used to treat wounds have to be biocompatible; therefore, the cytotoxicity indicator is frequently used to assess how well a material satisfies this crucial need. SEM images of PLA, PLA+Cur, and PLA+Cur+xAgNPs nanofibrous samples after cell culture are presented in Figures 7a-e, respectively. As it is evident from Figure 7a, cells exhibited a spindle-like shape as they adhered to and spread across the PLA-based wound dressings, firmly anchoring themselves onto the nanofibrous scaffolds. Furthermore, Figures 7b-e reveal that the addition of curcumin and silver nanoparticles, respectively, led to increased cell expansion and more comprehensive coverage of the nanofibrous, so that in a higher percentage of nanoparticles, a significant portion of the nanofibrous surfaces became enveloped by cells, resulting in the formation of multiple layers of cells on the fibrous. The graph also showed there was no significant difference ($p > 0.05$) between cell survival of PLA nanofibrous samples without AgNPs and with a low amount of AgNPs (Fig. 7). However, there is a significant difference ($p < 0.05$) observed between PLA and PLA+Cur+3%AgNPs nanofibrous samples for cell viability. In a comparable manner, Zhaonan Li et al. [58] demonstrated that, as compared to the PLA and PLA-4%AgNPs samples, the viable cells of CCC-HPF-1 cells on the PLA-6%AgNPs sample were the lowest numerous ($P < 0.0005$). The PLA-6%AgNPs and PLA samples exhibited significant differences, whereas the PLA-4 %AgNPs and PLA samples showed no differences, according to their live/dead test findings. Studies have revealed that Cur-AgNPs exhibit low cytotoxicity while promoting proliferation, migration, and collagen production in human dermal fibroblasts [47, 48].

Beyond the materials employed in scaffold construction, the morphology and structure of the fibers profoundly affect the behavior of the cells. The electrospinning method is a specialized technique

extensively utilized in wound healing applications, producing fibrous structures in the nano and micro ranges, as well as forming fibrous structures with a hollow structure, making it valuable in the realms of drug delivery and gene therapy. The size and positioning of the cavities on electrospun fibrous scaffolds are the key and influential factors in facilitating adhesion, proliferation, cell differentiation, and protein binding [47, 48]. It has been shown that electrospun nanofibers exhibit superior capabilities for cell growth, adhesion, and migration into the inner spaces of 3D porous scaffolds compared to many castable films [49]. The effects of curcumin and silver nanoparticles on cell growth and proliferation have also been documented by researchers in various studies. Previous experimental investigations on electrospun nanofibrous scaffolds incorporating silver nanoparticles have shown their significant role in facilitating cell absorption, proliferation, and growth [6, 11, 16, 50]. In the case of curcumin, while similar positive effects on cell adhesion and proliferation have been reported, its cytotoxic activity towards various cell types depends on both the dosage and the specific cell line [51, 52]. Furthermore, past research findings indicate that the combination of silver nanoparticles with other antibacterial agents has positive synergistic effects on cell behavior [53-58].

Fig. 7.

4. Conclusions

In the present study, PLA, PLA+Cur, PLA+Cur+1%AgNPs, PLA+Cur+2%AgNPs, and PLA+Cur+3%AgNPs nanofibrous scaffolds were fabricated using the electrospinning method for use as wound dressings. Investigations conducted using a scanning electron microscope revealed fibrous diameters ranging between 135 and 239 nm, with no beads and a uniform distribution in all nanofibrous samples. Due to the hydrophobic nature of PLA and curcumin, coupled with the characteristics of AgNPs, the results of the water absorption test showed values ranging between 0.0 and 0.25%, indicating negligible water absorption. The drug release test revealed that in the majority of samples, the release of curcumin exhibited a notable increase after 4 h, followed by relative stability over longer durations. The presence of curcumin enhances the tensile strength of the samples, while the presence of AgNPs decreases it. In the antibacterial evaluation, the presence of curcumin (84.06%) and the presence of AgNPs with curcumin (99.12%) exhibited effective bacteria destruction. In the MTT evaluation, the nanofibrous samples displayed no significant difference ($p > 0.05$) between cell survival of PLA nanofibrous samples without AgNPs and with a low amount of AgNPs (PLA+Cur+1%AgNPs) were observed. However, there is a significant

difference ($p < 0.05$) observed between PLA and PLA+Cur+3%AgNPs nanofibrous samples for cell viability. Taken together, our research's findings lend credence to the idea that encapsulation of Cur+AgNPs into PLA nanofibers is a viable approach for improving biocompatibility and antibacterial performance for use in burn treatment and wound healing.

References

[1] Chen S, Tian H, Mao J, Ma F, Zhang M, Chen F, et al. Preparation and application of chitosan-based medical electrospun nanofibers. International Journal of Biological Macromolecules. 2023;226: 410-22.

[2] Zhang M, Xu S, Wang R, Che Y, Han C, Feng W, et al. Electrospun nanofiber/hydrogel composite materials and their tissue engineering applications. Journal of Materials Science & Technology. 2023; 162:157-78.

[3] Deng S, Chen A, Chen W, Lai J, Pei Y, Wen J, et al. Fabrication of biodegradable and biocompatible functional polymers for anti-infection and augmenting wound repair. Polymers. 2023; 15(1): 120.

[4] Gul A, Gallus I, Tegginamath A, Maryska J, Yalcinkaya F. Electrospun antibacterial nanomaterials for wound dressings applications. Membranes. 2021; 11(12): 908.

[5] Parham S, Kharazi AZ, Bakhsheshi-Rad HR, Ghayour H, Ismail AF, Nur H, et al. Electrospun nano-fibers for biomedical and tissue engineering applications: A comprehensive review. Materials. 2020; 13(9): 2153.

[6] Hajikhani M, Emam-Djomeh Z, Askari G. Fabrication and characterization of mucoadhesive bioplastic patch via coaxial polylactic acid (PLA) based electrospun nanofibers with antimicrobial and wound healing application. International Journal of Biological Macromolecules. 2021;172: 143-53.

[7] El-Aassar MR, Ibrahim OM, Al-Oanzi ZH. Biotechnological applications of polymeric nanofiber platforms loaded with diverse bioactive materials. Polymers. 2021; 13(21): 3734.

[8] Kamaraj M, Moghimi N, Chen J, Morales R, Chen S, Khademhosseini A, et al. New dimensions of electrospun nanofiber material designs for biotechnological uses. Trends in Biotechnology. 2023.

[9] Syed MH, Khan MMR, Zahari MAKM, Beg MDH, Abdullah N. A review on current trends and future prospectives of electrospun biopolymeric nanofibers for biomedical applications. European Polymer Journal. 2023;197:112352.

[10] Pacheco KML, Torres BBM, Sanfelice RC, da Costa MM, Assis L, Marques RB, et al. Chitosan and chitosan/turmeric-based membranes for wound healing: Production, characterization and application. International Journal of Biological Macromolecules. 2023;253:127425.

[11] Perumal G, Pappuru S, Chakraborty D, Maya Nandkumar A, Chand DK, Doble M. Synthesis and characterization of curcumin loaded PLA—Hyperbranched polyglycerol electrospun blend for wound dressing applications. Materials Science and Engineering: C. 2017;76:1196-204.

[12] Akbik D, Ghadiri M, Chrzanowski W, Rohanizadeh R. Curcumin as a wound healing agent. Life Sciences. 2014;116(1):1-7.

[13] Sood A, Dev A, Das SS, Kim HJ, Kumar A, Thakur VK, et al. Curcumin-loaded alginate hydrogels for cancer therapy and wound healing applications: A review. International Journal of Biological Macromolecules. 2023;232:123283.

[14] Kumari M, Nanda DK. Potential of Curcumin nanoemulsion as antimicrobial and wound healing agent in burn wound infection. Burns. 2023;49(5):1003-16.

[15] Mohanty C, Sahoo SK. Curcumin and its topical formulations for wound healing applications. Drug Discovery Today. 2017;22(10):1582-92.
[16] Mitra S, Mateti T, Ramakrishna S, Laha A. A Review on Curcumin-Loaded Electrospun Nanofibers and their Application in Modern Medicine. JOM. 2022;74(9):3392-407.
[17] Choudhury H, Pandey M, Lim YQ, Low CY, Lee CT, Marilyn TCL, et al. Silver nanoparticles: Advanced and promising technology in diabetic wound therapy. Materials Science and Engineering: C. 2020; 112:110925.
[18] Bakhsheshi-Rad HR, Ismail AF, Aziz M, Akbari M, Hadisi Z, Khoshnava SM, et al. Co-incorporation of graphene oxide/silver nanoparticle into poly-L-lactic acid fibrous: A route toward the development of cytocompatible and antibacterial coating layer on magnesium implants. Materials Science and Engineering: C. 2020;111:110812.
[19] Khan MR, Urmi MA, Kamaraj C, Malafaia G, Ragavendran C, Rahman MM. Green synthesis of silver nanoparticles with its bioactivity, toxicity and environmental applications: A comprehensive literature review. Environmental Nanotechnology, Monitoring & Management. 2023;20:100872.
[20] Kumar M, Mahmood S, Chopra S, Bhatia A. Biopolymer based nanoparticles and their therapeutic potential in wound healing – A review. International Journal of Biological Macromolecules. 2024; 267:131335.
[21] Magdy G, Aboelkassim E, Abd Elhaleem SM, Belal F. A comprehensive review on silver nanoparticles: Synthesis approaches, characterization techniques, and recent pharmaceutical, environmental, and antimicrobial applications. Microchemical Journal. 2024;196:109615.
[22] Vishwanath R, Negi B. Conventional and green methods of synthesis of silver nanoparticles and their antimicrobial properties. Current Research in Green and Sustainable Chemistry. 2021;4: 100205.
[23] Fu X, Rehman U, Wei L, Chen Z-S, Abourehab MAS, Kesharwani P, et al. Silver-dendrimer nanocomposite as emerging therapeutics in anti-bacteria and beyond. Drug Resistance Updates. 2023;68:100935.
[24] Azizi-Lalabadi M, Garavand F, Jafari SM. Incorporation of silver nanoparticles into active antimicrobial nanocomposites: Release behavior, analyzing techniques, applications and safety issues. Advances in Colloid and Interface Science. 2021;293:102440.
[25] Safarpour F, Kharaziha M, Emadi R. Inspiring biomimetic system based on red blood cell membrane vesicles for effective curcumin loading and release. International Journal of Pharmaceutics. 2022;613:121419.
[26] Ghaee A, Bagheri-Khoulenjani S, Amir Afshar H, Bogheiri H. Biomimetic nanocomposite scaffolds based on surface modified PCL-nanofibers containing curcumin embedded in chitosan/gelatin for skin regeneration. Composites Part B: Engineering. 2019;177:107339.
[27] Li D, Jiang Y, Lv S, Liu X, Gu J, Chen Q, et al. Preparation of plasticized poly (lactic acid) and its influence on the properties of composite materials. PLOS ONE. 2018;13(3):e0193520.
[28] Arunraj TR, Sanoj Rejinold N, Ashwin Kumar N, Jayakumar R. Bio-responsive chitin-poly(l-lactic acid) composite nanogels for liver cancer. Colloids and Surfaces B: Biointerfaces. 2014;113:394-402.
[29] Roshanghias A, Sodeifian G, Javidparvar AA, Tarashi S. Construction of a novel polytetrafluoroe thylene-based sealant paste: The effect of polyvinyl butyral (PVB) and nano-alumina on the sealing performance and construction formulations. Results in Engineering. 2022;14:100460.
[30] Ramli RH, Fhong Soon C, Mohd Rus AZ. Synthesis of chitosan/alginate/silver nanoparticles hydrogel scaffold. MATEC Web Conf. 2016;78.

[31] Luz PP, e Silva MLA, Hinestroza JP. Curcumin-loaded biodegradable electrospun fibers: preparation, characterization, and differences in fiber morphology. International Journal of Polymer Analysis and Characterization. 2013;18(7):534-44.
[32] Ahmadi T, Monshi A, Mortazavi V, Fathi MH, Sharifi S, Kharaziha M, et al. Fabrication and characterization of polycaprolactone fumarate/gelatin-based nanocomposite incorporated with silicon and magnesium co-doped fluorapatite nanoparticles using electrospinning method. Materials Science and Engineering: C. 2020;106:110172.
[33] Bardania H, Mahmoudi R, Bagheri H, Salehpour Z, Fouani MH, Darabian B, et al. Facile preparation of a novel biogenic silver-loaded Nanofilm with intrinsic anti-bacterial and oxidant scavenging activities for wound healing. Scientific Reports. 2020;10(1):6129.
[34] Krishnamohan S, Anandaram H, Rathinam V, Kaliappan S, Sekar S, Patil PP, et al. Optimization of water absorption and mechanical and thermal behavior of polylactic acid/chitosan/titanium carbide. Advances in Materials Science and Engineering. 2022;2022: 5176584.
[35] Sarma R, Das M, Saikia L, Ramteke A, Saikia R. Conjugation of curcumin with Ag nanoparticle for improving its bioavailability and study of the bioimaging response. Nanosystems: Physics, Chemistry, Mathematics. 2021;12:528-35.
[36] Farazin A, Mohammadimehr M, Ghasemi AH, Naeimi H. Design, preparation, and characterization of CS/PVA/SA hydrogels modified with mesoporous Ag_2O/SiO_2 and curcumin nanoparticles for green, biocompatible, and antibacterial biopolymer film. RSC Advances. 2021;11(52):32775-91.
[37] Sharifah ISS, Qairol AAB, Azlina HN, Khairusshima MKN. Thermal, structural and mechanical properties of melt drawn Cur-loaded poly(lactic acid) fibers. Procedia Engineering. 2017;184:544-51.
[38] Izadi R, Trovalusci P, Fantuzzi N. A study on the effect of doping metallic nanoparticles on fracture properties of polylactic acid nanofibres via molecular dynamics simulation. Nanomaterials. 2023; 13(6): 989.
[39] He M, Chen M, Dou Y, Ding J, Yue H, Yin G, et al. Electrospun silver nanoparticles-embedded feather keratin/poly(vinyl alcohol)/poly(ethylene oxide) antibacterial composite nanofibers. Polymers. 2020; 12(2): 305.
[40] Song Y, Hu Q, Liu S, Wang Y, Zhang H, Chen J, et al. Electrospinning/3D printing drug-loaded antibacterial polycaprolactone nanofiber/sodium alginate-gelatin hydrogel bilayer scaffold for skin wound repair. International Journal of Biological Macromolecules. 2024:129705.
[41] Xie H, Ouyang K, Zhang L, Hu J, Huang S, Sun W, et al. Chitosan/rice hydrolysate/curcumin composite film: Effect of chitosan molecular weight. International Journal of Biological Macromolecules. 2022;210:53-62.
[42] Liu S, Zhao J, Ruan H, Wang W, Wu T, Cui W, et al. Antibacterial and anti-adhesion effects of the silver nanoparticles-loaded poly(l-lactide) fibrous membrane. Materials Science and Engineering: C. 2013;33(3):1176-82.
[43] Pishbin F, Mouriño V, Gilchrist JB, McComb DW, Kreppel S, Salih V, et al. Single-step electrochemical deposition of antimicrobial orthopaedic coatings based on a bioactive glass/chitosan/ nano-silver composite system. Acta Biomaterialia. 2013;9(7):7469-79.
[44] Akshaykranth A, Jayarambabu N, kumar A, Venkatappa Rao T, Kumar RR, Srinivasa Rao L. Novel nanocomposite polylactic acid films with Curcumin-ZnO: structural, thermal, optical and antibacterial properties. Current Research in Green and Sustainable Chemistry. 2022;5:100332.
[45] Wang Q, Liu S, Lu W, Zhang P. Fabrication of Curcumin@Ag Loaded Core/Shell Nanofiber Membrane and its Synergistic Antibacterial Properties. Frontiers in Chemistry. 2022;10.

[46] El-Kattan N, Emam AN, Mansour AS, Ibrahim MA, Abd El-Razik AB, Allam KAM, et al. Curcumin assisted green synthesis of silver and zinc oxide nanostructures and their antibacterial activity against some clinical pathogenic multi-drug resistant bacteria. RSC Advances. 2022; 12(28): 18022-38.
[47] Bhubhanil S, Talodthaisong C, Khongkow M, Namdee K, Wongchitrat P, Yingmema W, et al. Enhanced wound healing properties of guar gum/curcumin-stabilized silver nanoparticle hydrogels. Scientific Reports. 2021;11(1):21836.
[48] Madivoli ES, Kareru PG, Gichuki J, Elbagoury MM. Cellulose nanofibrils and silver nanoparticles enhances the mechanical and antimicrobial properties of polyvinyl alcohol nanocomposite film. Scientific Reports. 2022;12(1):19005.
[49] Liu C, Zhu Y, Lun X, Sheng H, Yan A. Effects of wound dressing based on the combination of silver @curcumin nanoparticles and electrospun chitosan nanofibers on wound healing. Bioengineered. 2022;13(2):4328-39.
[50] Alven S, Buyana B, Feketshane Z, Aderibigbe BA. Electrospun nanofibers/nanofibrous scaffolds loaded with silver nanoparticles as effective antibacterial wound dressing materials. Pharmaceutics. 2021; 13(7): 964.
[51] Akrami-Hasan-Kohal M, Tayebi L, Ghorbani M. Curcumin-loaded naturally-based nanofibers as active wound dressing mats: morphology, drug release, cell proliferation, and cell adhesion studies. New Journal of Chemistry. 2020;44(25):10343-51.
[52] Júnior AF, Ribeiro CA, Leyva ME, Marques PS, Soares CRJ, Alencar de Queiroz AA. Biophysical properties of electrospun chitosan-grafted poly(lactic acid) nanofibrous scaffolds loaded with chondroitin sulfate and silver nanoparticles. Journal of Biomaterials Applications. 2021;36(6): 1098-110.
[53] Hashemi S-S, Saadatjo Z, Mahmoudi R, Delaviz H, Bardania H, Rajabi S-S, et al. Preparation and evaluation of polycaprolactone/chitosan/Jaft biocompatible nanofibers as a burn wound dressing. Burns. 2022;48(7):1690-705.
[54] Li S, Liu Y, Huang Z, Kou Y, Hu A. Efficacy and safety of nano-silver dressings combined with recombinant human epidermal growth factor for deep second-degree burns: A meta-analysis. Burns. 2021;47(3):643-53.
[55] G. El Baassiri M, Dosh L, Haidar H, Gerges A, Baassiri S, Leone A, et al. Nerve growth factor and burn wound healing: Update of molecular interactions with skin cells. Burns. 2023;49(5):989-1002.
[56] Rangatchew F, Vester-Glowinski P, Rasmussen BS, Haastrup E, Munthe-Fog L, Talman M-L, et al. Mesenchymal stem cell therapy of acute thermal burns: A systematic review of the effect on inflammation and wound healing. Burns. 2021;47(2):270-94.
[57] Knoz M, Holoubek J, Lipový B, Faldyna M, Chaloupková R, Pavliňáková V, et al. Evaluation of viscoelastic parameters and photo-based assessment of newly developed dermal substitutes modified with thermostabilized fibroblast growth factor 2. Burns. 2024.
[58] Li Z, Jiao D, Zhang W, Ren K, Qiu L, Tian C, Li Y, Li J, Zhou X, Zhao Y, Han X. Antibacterial and antihyperplasia polylactic acid/silver nanoparticles nanofiber membrane-coated airway stent for tracheal stenosis. Colloids and Surfaces B: Biointerfaces. 2021;206:111949.